Theoretical model for the afterglow of Gamma-Ray Bursts

Federico Fraschetti

CEA/Saclay, DSM/Dapnia/Service d'Astrophysique

and Physics Department, University of Rome 'La Sapienza'

R. Ruffini, C.L.Bianco, P.Chardonnet, M.G.Bernardini, R. Guida, S.S. Xue

"Physics of the Universe Confronts Observations", Rencontre at the Colegio de España , May 18 2007

Theoretical model for the afterglow of Gamma-Ray Bursts

Federico Fraschetti

CEA/Saclay, DSM/Dapnia/Service d'Astrophysique

and Physics Department, University of Rome 'La Sapienza'

R. Ruffini, C.L.Bianco, P.Chardonnet, M.G.Bernardini, R. Guida, S.S. Xue

"Physics of the Universe Confronts Observations", Rencontre at the Colegio de España , May 18 2007

Theoretical model for the afterglow of Gamma-Ray Bursts

Federico Fraschetti

CEA/Saclay, DSM/Dapnia/Service d'Astrophysique

and Physics Department, University of Rome 'La Sapienza'

R. Ruffini, C.L.Bianco, P.Chardonnet, M.G.Bernardini, R. Guida, S.S. Xue

"Physics of the Universe Confronts Observations", Rencontre at the Colegio de España , May 18 2007

Theoretical model for the afterglow of Gamma-Ray Bursts

Federico Fraschetti

CEA/Saclay, DSM/Dapnia/Service d'Astrophysique

and Physics Department, University of Rome 'La Sapienza'

R. Ruffini, C.L.Bianco, P.Chardonnet, M.G.Bernardini, R. Guida, S.S. Xue

"Physics of the Universe Confronts Observations", Rencontre at the Colegio de España , May 18 2007

Summary

- Discovery

Summary

- Discovery
- Key Observations

Summary

- Discovery
- Key Observations
- Model: assumptions, parameters, equations

Summary

- Discovery
- Key Observations
- Model: assumptions, parameters, equations
- Application to GRB 991216, GRB 980425, GRB 031203…

Summary

- Discovery
- Key Observations
- Model: assumptions, parameters, equations
- Application to GRB 991216, GRB 980425, GRB 031203…
- Main results :

    Interpretation of temporal structure of GRBs.

    Relation between inhomogeneities of ISM and temporal variability of light curve.

    Thermal distribution of radiation in comoving system of the expanding plasma.

    Canonical X-ray afterglow light curve of Swift

    Short burst.

Discovery of GRBs

•GRBs unknown until the end of ‘60 neither predicted by astrophysical or cosmological models

Discovery of GRBs

•GRBs unknown until the end of '60 neither predicted by astrophysical or cosmological models

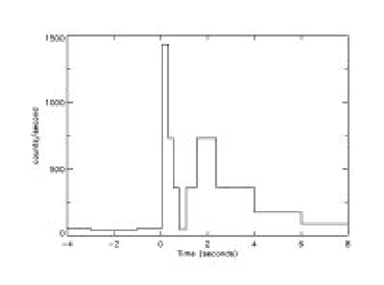

•Discovery by chance by *Vela* satellite (1973)

Discovery of GRBs

•GRBs unknown until the end of ‘60 neither predicted by astrophysical or cosmological models

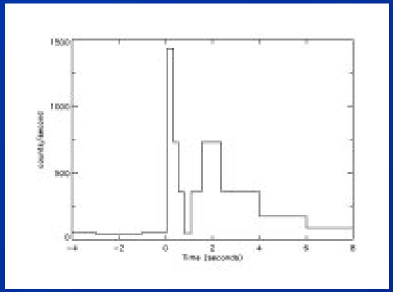

•Discovery by chance by *Vela* satellite (1973)

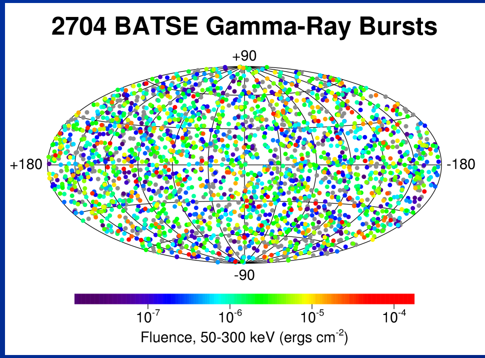

•I revolution (*BATSE* satellite, ‘90):

isotropy of spatial distribution

Discovery of GRBs

•GRBs unknown until the end of ‘60 neither predicted by astrophysical or cosmological models

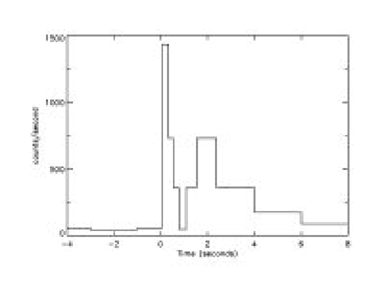

•Discovery by chance by *Vela* satellite (1973)

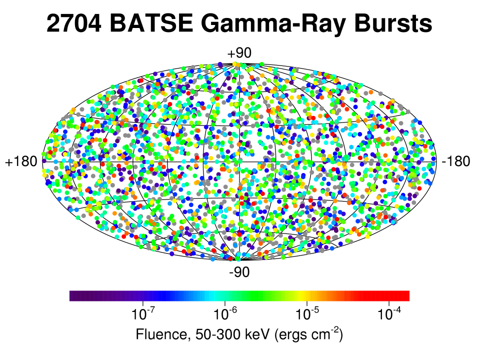

•I revolution (*BATSE* satellite, ‘90):

isotropy of spatial distribution

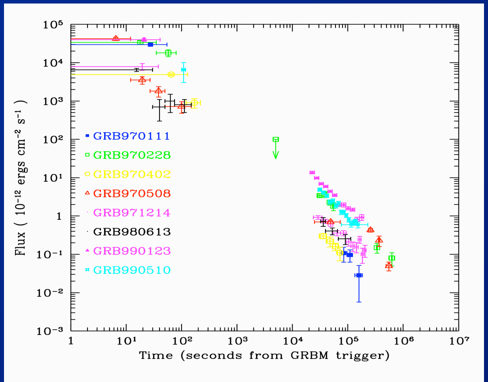

•II revolution (BeppoSAX, 1997):

1. discovery of **afterglow** *X*
2. cosmological distance (z order of 1)

Observations

•**Irregularity** of temporal profile of single event and **variability** of temporal profile between different events

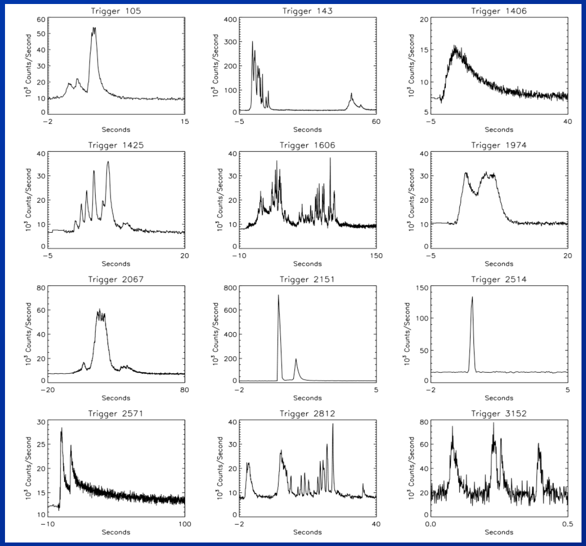

Observations

•**Irregularity** of temporal profile of single event and **variability** of temporal profile between different events

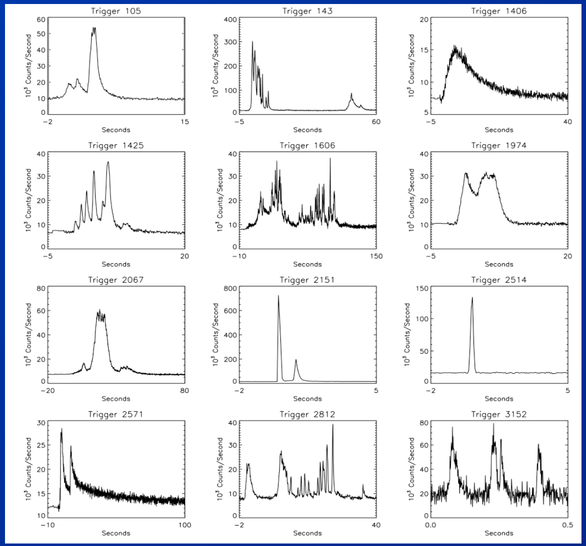

•**Bimodal** distribution of duration

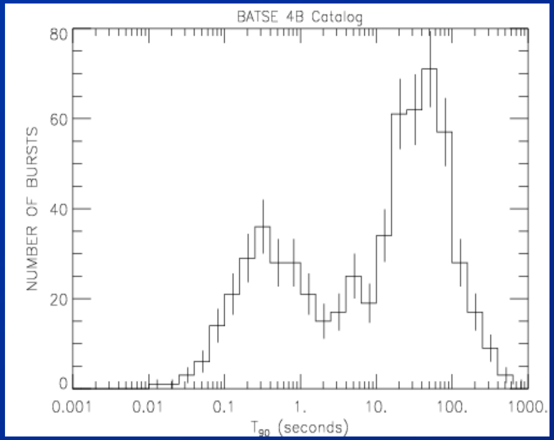

Observations

•**Irregularity** of temporal profile of single event and **variability** of temporal profile between different events

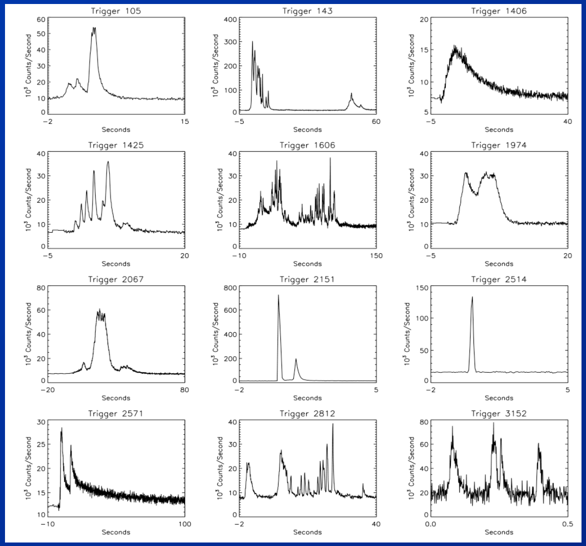

•**Bimodal** distribution of duration

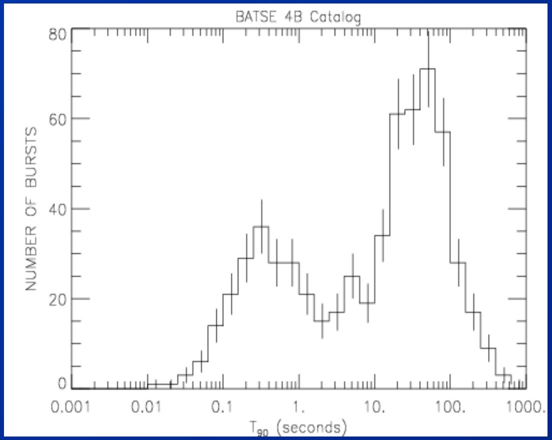

•**Observed** spectrum non-thermal..

Theoretical model

GRBs originate from the vacuum polarization process *á la* Heisenberg-Euler-Schwinger in the space-time surrounding a non-rotating electromagnetic black hole

Theoretical model

GRBs originate from the vacuum polarization process *á la* Heisenberg-Euler-Schwinger in the space-time surrounding a non-rotating electromagnetic black hole

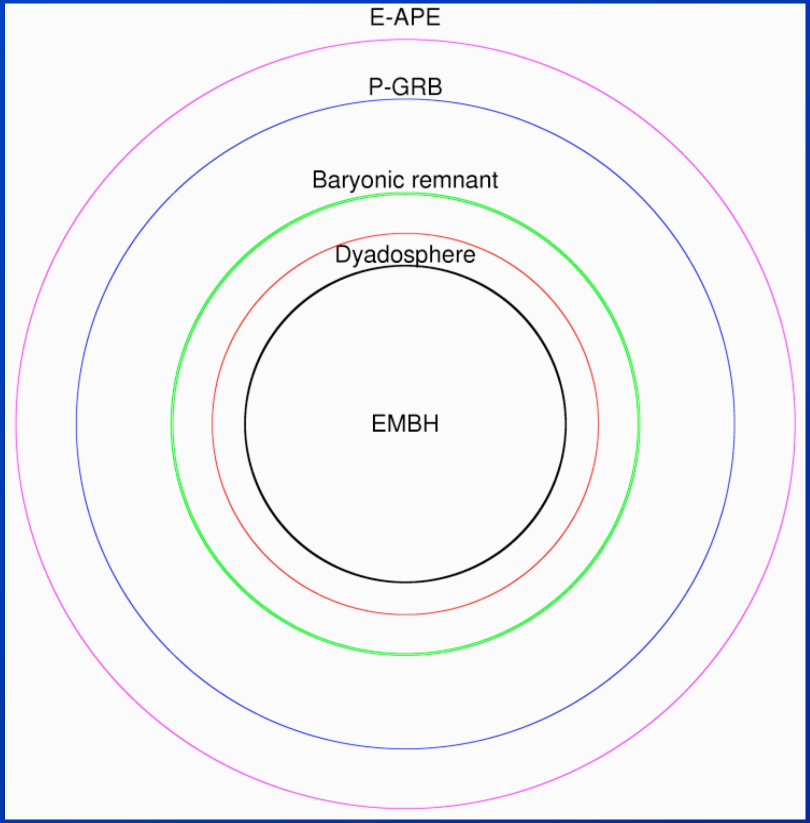

Theoretical model

GRBs originate from the vacuum polarization process *á la* Heisenberg-Euler-Schwinger in the space-time surrounding a non-rotating electromagnetic black hole

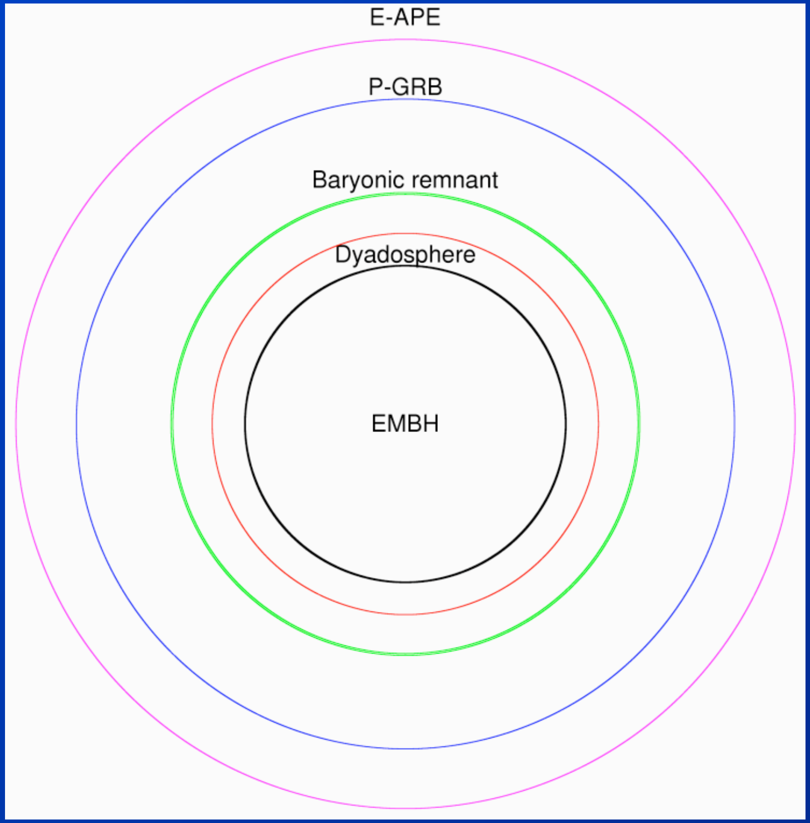

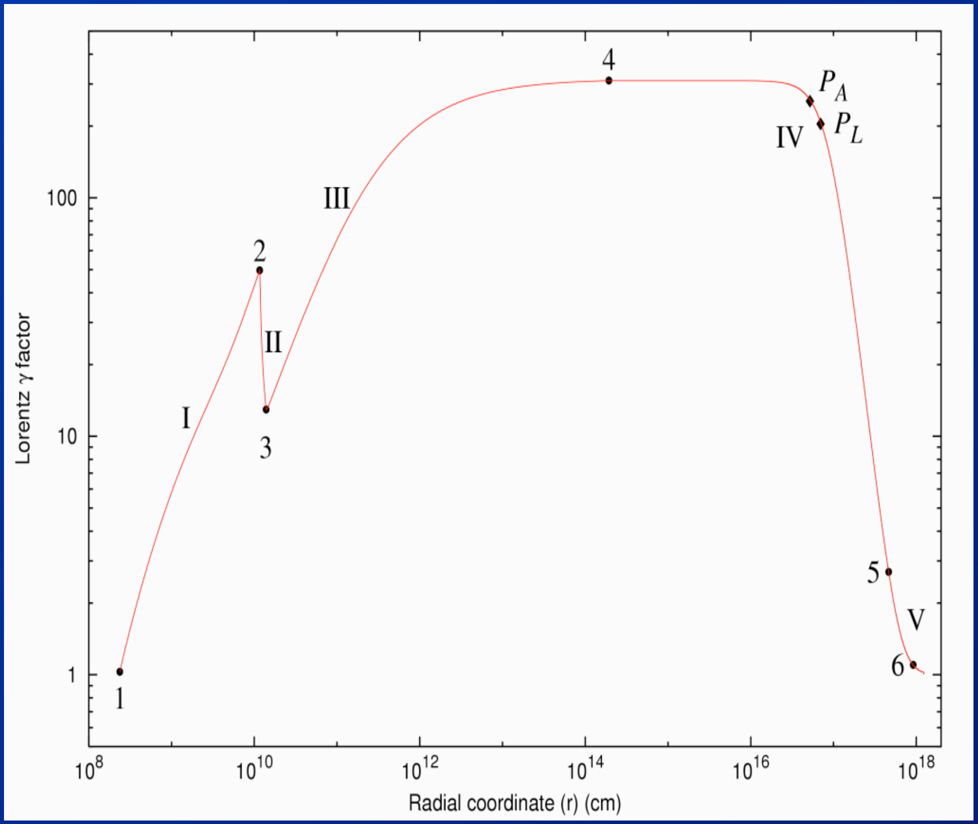

Theoretical model

GRBs originate from the vacuum polarization process *á la* Heisenberg-Euler-Schwinger in the space-time surrounding a non-rotating electromagnetic black hole

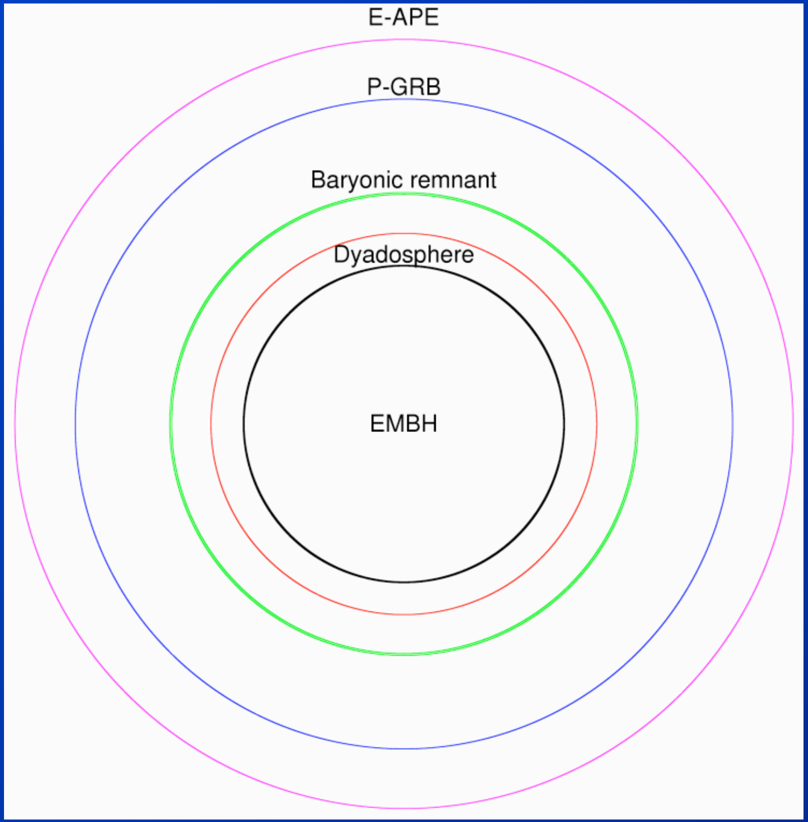

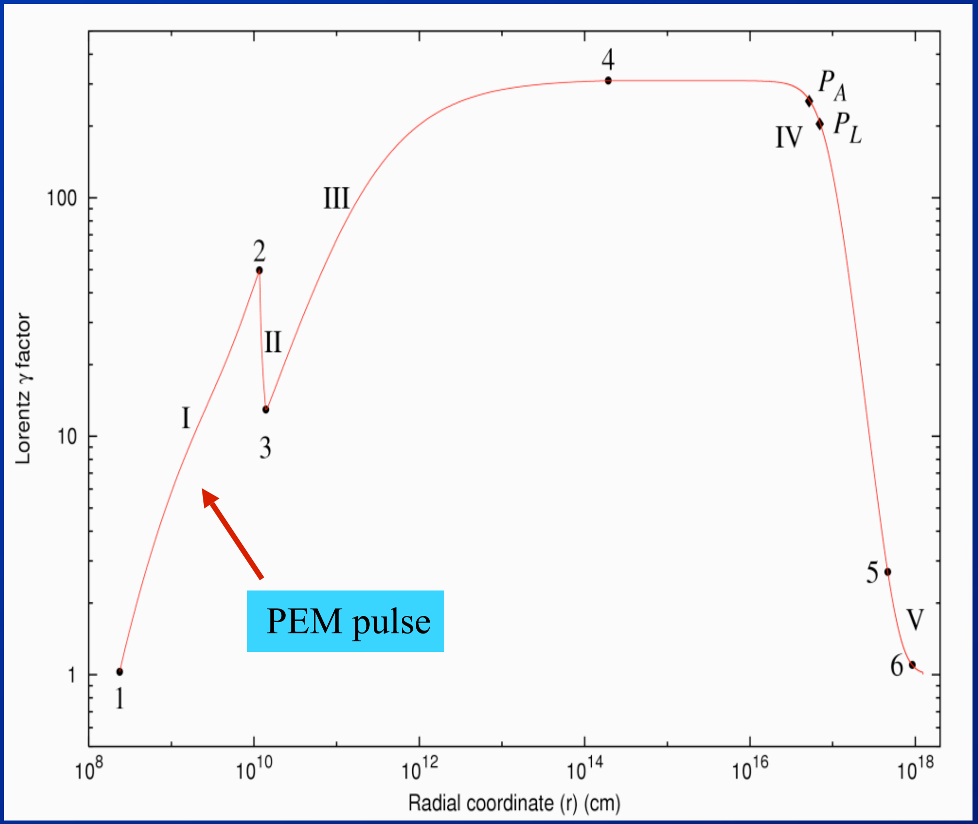

Theoretical model

GRBs originate from the vacuum polarization process *á la* Heisenberg-Euler-Schwinger in the space-time surrounding a non-rotating electromagnetic black hole

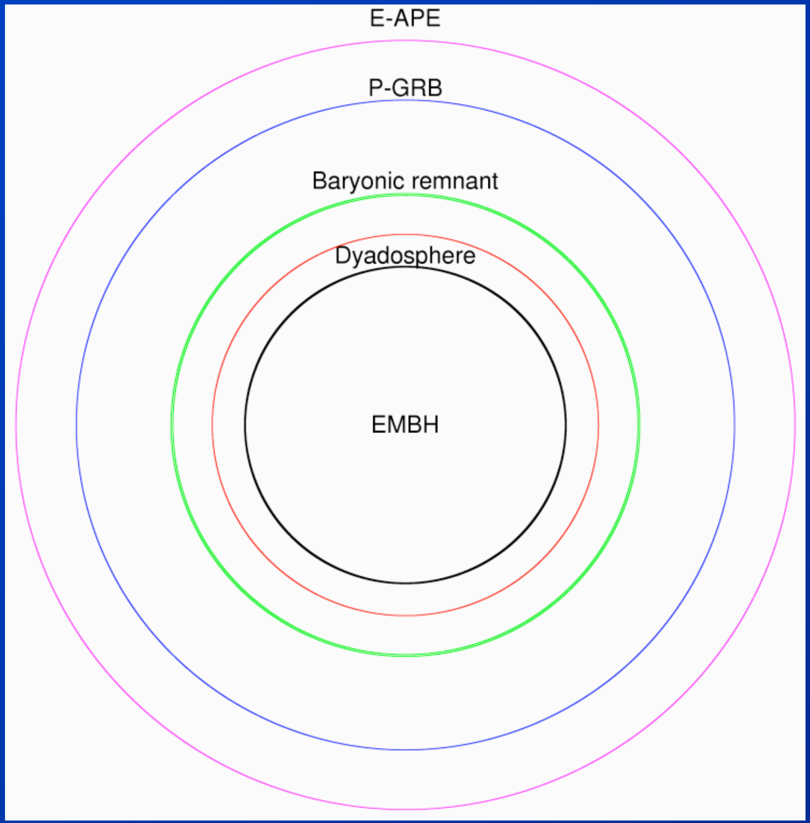

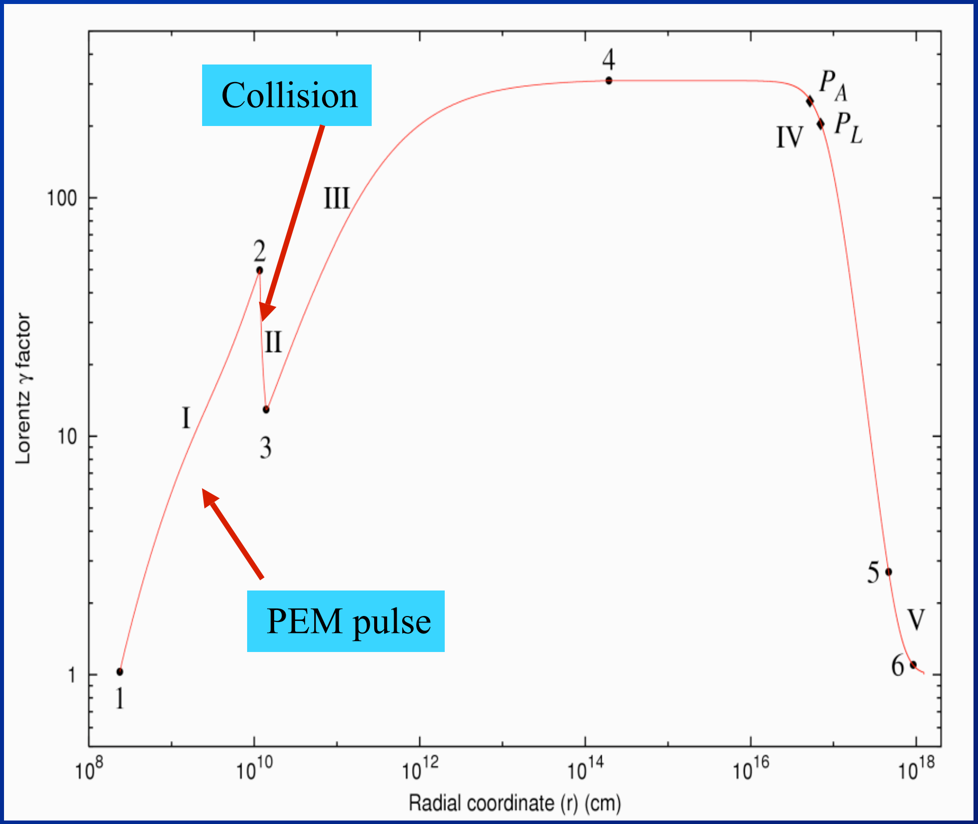

Theoretical model

GRBs originate from the vacuum polarization process *á la* Heisenberg-Euler-Schwinger in the space-time surrounding a non-rotating electromagnetic black hole

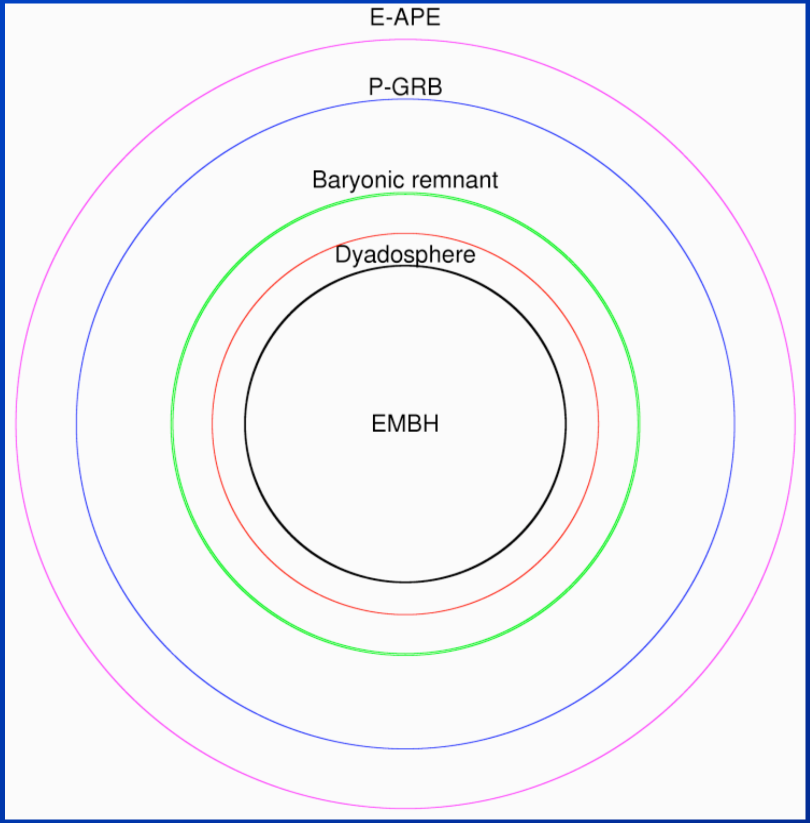

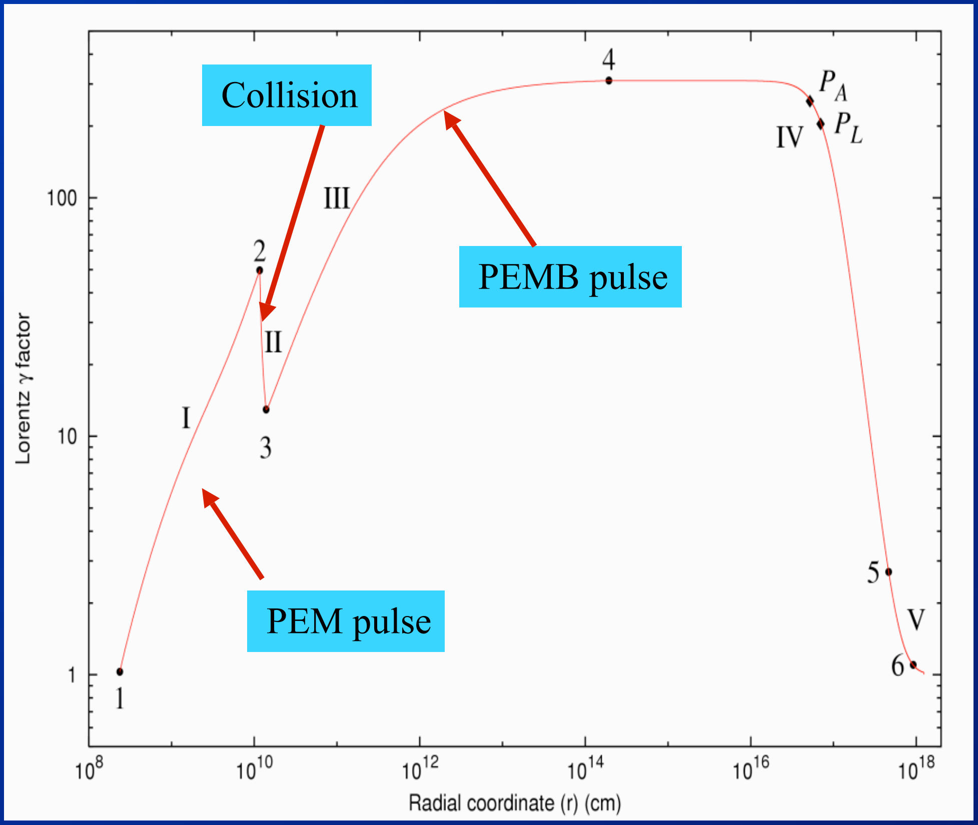

Theoretical model

GRBs originate from the vacuum polarization process *á la* Heisenberg-Euler-Schwinger in the space-time surrounding a non-rotating electromagnetic black hole

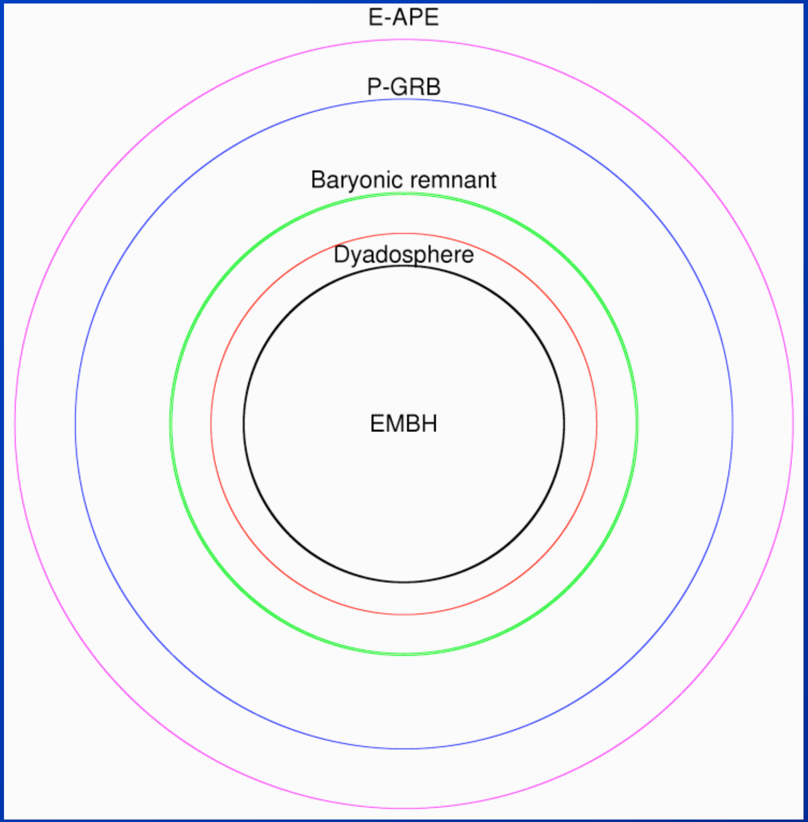

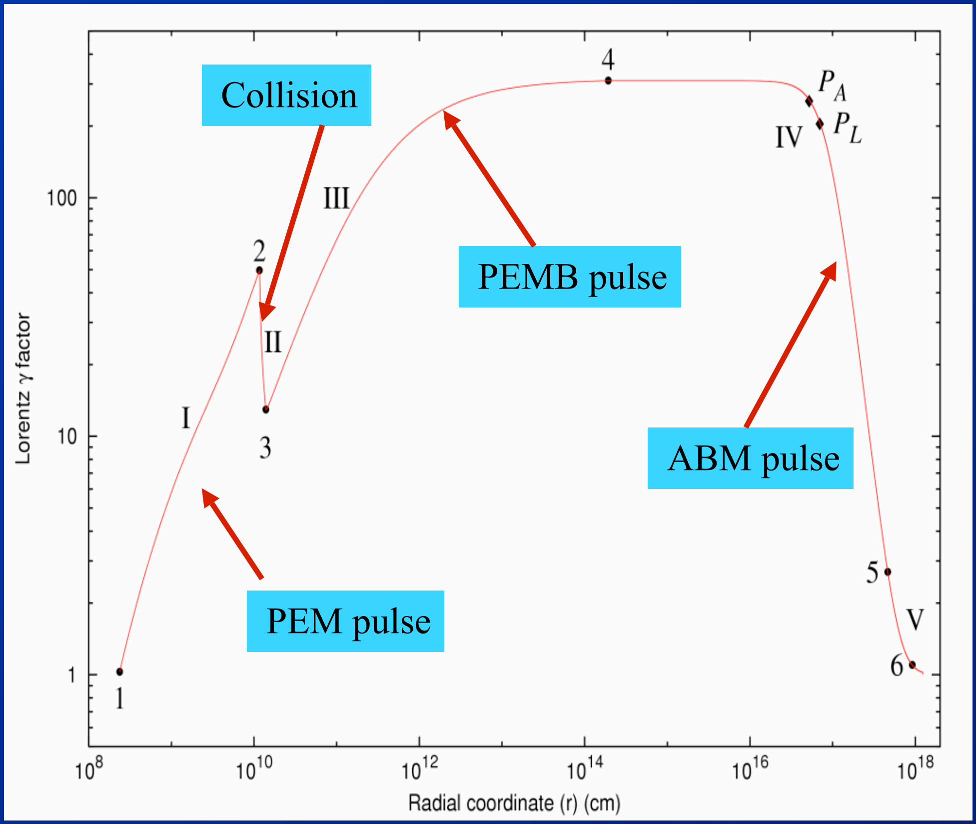

Theoretical model

GRBs originate from the vacuum polarization process *á la* Heisenberg-Euler-Schwinger in the space-time surrounding a non-rotating electromagnetic black hole

Point	$r(cm)$	$\tau(s)$	$t(s)$	$t_a(s)$	$t_a^d(s)$	γ	"Superluminal" $v \equiv \frac{r}{t_a^d}$
The Injector Phase							
1	2.354×10^{8}	0.0	0.0	0.0	0.0	1.000	0
	1.871×10^{9}	1.550×10^{-2}	5.886×10^{-2}	4.312×10^{-3}	8.625×10^{-3}	10.08	$7.23c$
	4.486×10^{9}	2.141×10^{-2}	1.463×10^{-1}	4.523×10^{-4}	9.046×10^{-3}	20.26	$16.5c$
	7.080×10^{9}	2.485×10^{-2}	2.329×10^{-1}	4.594×10^{-3}	9.187×10^{-3}	30.46	$25.7c$
	9.533×10^{9}	2.715×10^{-2}	3.148×10^{-1}	4.627×10^{-3}	9.253×10^{-3}	40.74	$34.4c$
	1.162×10^{10}	2.868×10^{-2}	3.845×10^{-1}	4.644×10^{-3}	9.288×10^{-3}	49.70	$41.7c$
2	1.162×10^{10}	2.868×10^{-2}	3.845×10^{-1}	4.644×10^{-3}	9.288×10^{-3}	49.70	$41.7c$
	1.186×10^{10}	2.889×10^{-2}	3.923×10^{-1}	4.646×10^{-3}	9.292×10^{-3}	38.06	$42.6c$
	1.234×10^{10}	2.949×10^{-2}	4.083×10^{-1}	4.655×10^{-3}	9.311×10^{-3}	24.21	$44.2c$
	1.335×10^{10}	3.144×10^{-2}	4.423×10^{-1}	4.706×10^{-3}	9.413×10^{-3}	15.14	$47.3c$
	1.389×10^{10}	3.279×10^{-2}	4.603×10^{-1}	4.753×10^{-3}	9.506×10^{-3}	12.94	$48.7c$
3	1.389×10^{10}	3.279×10^{-2}	4.603×10^{-1}	4.753×10^{-3}	9.506×10^{-3}	12.94	$48.7c$
	2.326×10^{10}	5.208×10^{-2}	7.733×10^{-1}	5.369×10^{-3}	1.074×10^{-2}	20.09	$72.2c$
	6.913×10^{10}	9.694×10^{-2}	2.304	6.086×10^{-3}	1.217×10^{-2}	50.66	$1.89 \times 10^{2}c$
	1.861×10^{11}	1.486×10^{-1}	6.206	6.446×10^{-3}	1.289×10^{-2}	100.1	$4.82 \times 10^{2}c$
	9.629×10^{11}	3.112×10^{-1}	32.12	6.978×10^{-3}	1.396×10^{-2}	200.3	$2.30 \times 10^{3}c$
	3.205×10^{13}	3.958	1.069×10^{3}	1.343×10^{-2}	2.685×10^{-2}	300.1	$3.98 \times 10^{4}c$
	1.943×10^{14}	21.57	6.481×10^{3}	4.206×10^{-2}	8.413×10^{-2}	310.1	$7.70 \times 10^{4}c$
The Beam-Target Phase							
4	1.943×10^{14}	21.57	6.481×10^{3}	4.206×10^{-2}	8.413×10^{-2}	310.1	$7.70 \times 10^{4}c$
	6.663×10^{15}	7.982×10^{2}	6.481×10^{3}	1.164	2.328	310.0	$9.55 \times 10^{4}c$
	2.863×10^{16}	3.114×10^{3}	9.549×10^{5}	5.057	10.11	300.0	$9.45 \times 10^{4}c$
	4.692×10^{16}	5.241×10^{3}	1.565×10^{6}	8.775	17.55	270.0	$8.92 \times 10^{4}c$
P_A	5.177×10^{16}	5.853×10^{3}	1.727×10^{6}	9.933	19.87	258.5	$8.69 \times 10^{4}c$
	5.878×10^{16}	6.791×10^{3}	1.961×10^{6}	11.82	23.63	240.0	$8.30 \times 10^{4}c$
	6.580×10^{16}	7.811×10^{3}	2.195×10^{6}	14.03	28.06	220.0	$7.82 \times 10^{4}c$
P_L	7.025×10^{16}	8.506×10^{3}	2.343×10^{6}	15.66	31.32	207.0	$7.48 \times 10^{4}c$
	7.262×10^{16}	8.895×10^{3}	2.422×10^{6}	16.61	33.23	200.0	$7.29 \times 10^{4}c$
	9.058×10^{16}	1.236×10^{4}	3.021×10^{6}	26.66	53.32	150.0	$5.67 \times 10^{4}c$
	1.136×10^{17}	1.866×10^{4}	3.788×10^{6}	52.84	1.057×10^{2}	100.0	$3.58 \times 10^{4}c$
	1.539×10^{17}	3.819×10^{4}	5.134×10^{6}	2.000×10^{2}	4.000×10^{2}	50.02	$1.28 \times 10^{4}c$
	2.801×10^{17}	2.622×10^{5}	9.351×10^{6}	7.278×10^{3}	1.455×10^{4}	10.00	$6.42 \times 10^{2}c$
	3.624×10^{17}	6.702×10^{5}	1.213×10^{7}	3.860×10^{4}	7.719×10^{4}	5.001	$1.57 \times 10^{2}c$
	4.454×10^{17}	1.433×10^{6}	1.500×10^{7}	1.439×10^{5}	2.877×10^{5}	2.998	$51.6c$
5	4.454×10^{17}	1.433×10^{6}	1.500×10^{7}	1.439×10^{5}	2.877×10^{5}	2.998	$51.6c$
	4.830×10^{17}	1.928×10^{6}	1.635×10^{7}	2.381×10^{5}	4.762×10^{5}	2.500	$33.8c$
	5.390×10^{17}	2.873×10^{6}	1.844×10^{7}	4.643×10^{5}	9.285×10^{5}	2.000	$19.4c$
	6.422×10^{17}	5.387×10^{6}	2.271×10^{7}	1.291×10^{6}	2.581×10^{6}	1.500	$8.30c$
	1.034×10^{18}	2.903×10^{7}	5.002×10^{7}	1.552×10^{7}	3.103×10^{7}	1.054	$1.11c$
6	1.034×10^{18}	2.903×10^{7}	5.002×10^{7}	1.552×10^{7}	3.103×10^{7}	1.054	$1.11c$
	1.202×10^{18}	4.979×10^{7}	7.150×10^{7}	3.140×10^{7}	6.280×10^{7}	1.025	$6.38 \times 10^{-1}c$
F	1.248×10^{18}	5.706×10^{7}	7.894×10^{7}	3.731×10^{7}	7.461×10^{7}	1.000	$5.58 \times 10^{-1}c$

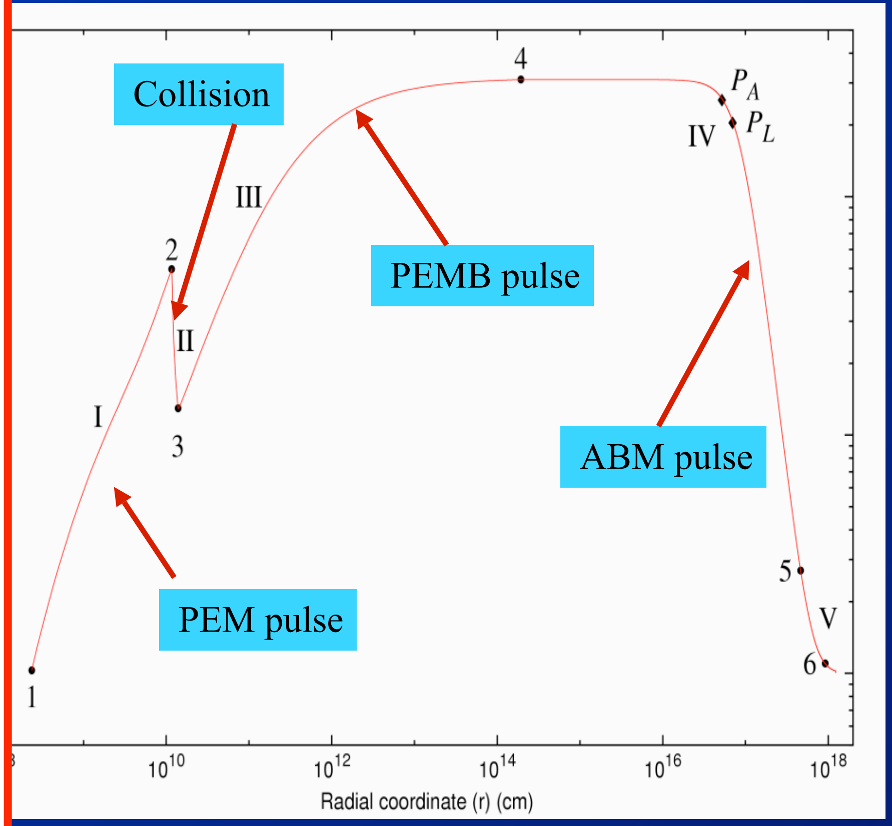

Ruffini R., Bianco C.L., Chardonnet P., Fraschetti F., Xue S.S., ApJ, 555, L107, 2001

Assumptions

Parameters of the model

Assumptions

Constant thickness in the laboratory system
Spherical symmetry
"Fully radiative" condition
Temporal variability of light curve due to inhomogeneity of interstellar medium
Thermal distribution of energy in comoving frame

Parameters of the model

Assumptions

Constant thickness in the laboratory system
Spherical symmetry
"Fully radiative" condition
Temporal variability of light curve due to inhomogeneity of interstellar medium
Thermal distribution of energy in comoving frame

Parameters of the model

E_{dya} is the total energy emitted by source
B= $M_B c^2/E_{dya}$ parametrizes baryonic matter protostellar not collapsed
$R = A_{eff}/A_{tot}$ indicates the porosity of interstellar medium
$\langle n_{ism} \rangle$ is the particle number density of interstellar medium

Temporal structure of GRB

Collision with baryonic remnant

Temporal structure of GRB

Collision with baryonic remnant

Increase of opacity of pulse

Temporal structure of GRB

Collision with baryonic remnant

Increase of opacity of pulse

Conversion of internal energy in kinetic energy

Temporal structure of GRB

Collision with baryonic remnant

Increase of opacity of pulse

Conversion of internal energy in kinetic energy

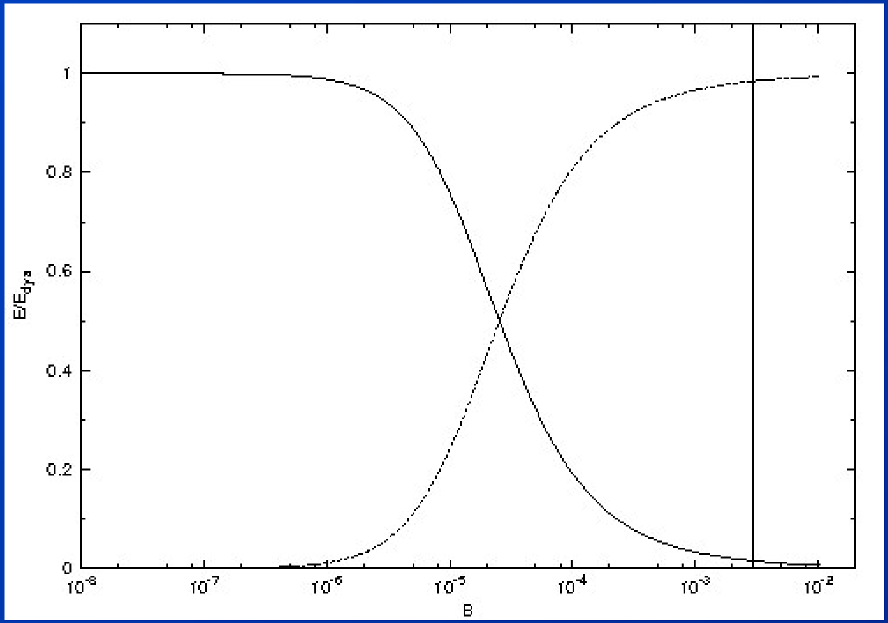

Temporal structure of GRB

Collision with baryonic remnant

Increase of opacity of pulse

Conversion of internal energy in kinetic energy

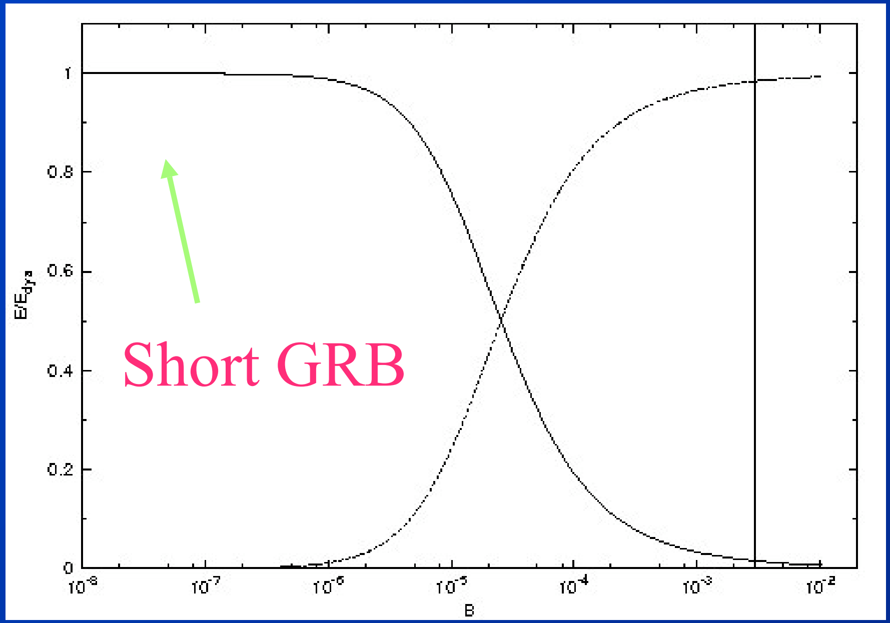

Temporal structure of GRB

Collision with baryonic remnant

Increase of opacity of pulse

Conversion of internal energy in kinetic energy

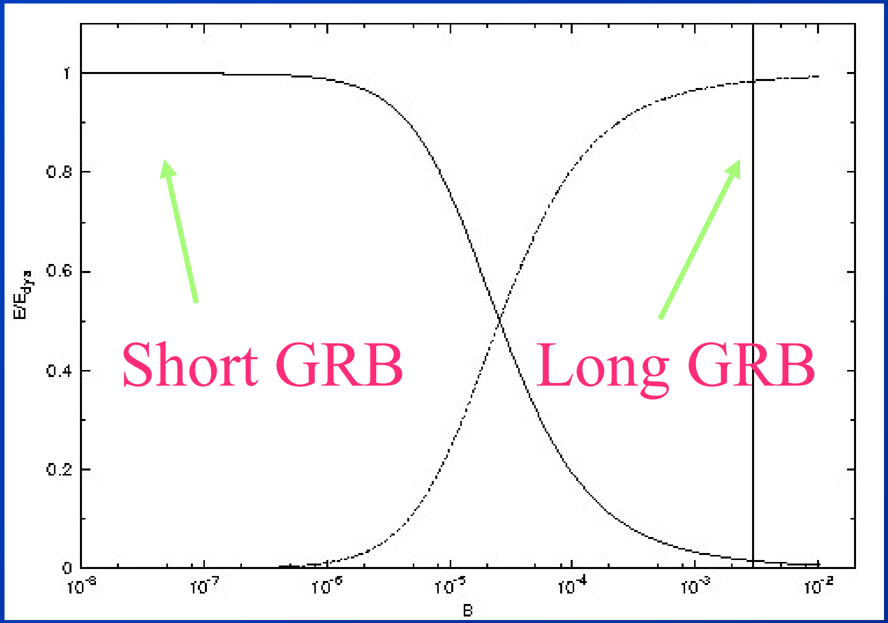

Temporal structure of GRB

Collision with baryonic remnant

Increase of opacity of pulse

Conversion of internal energy in kinetic energy

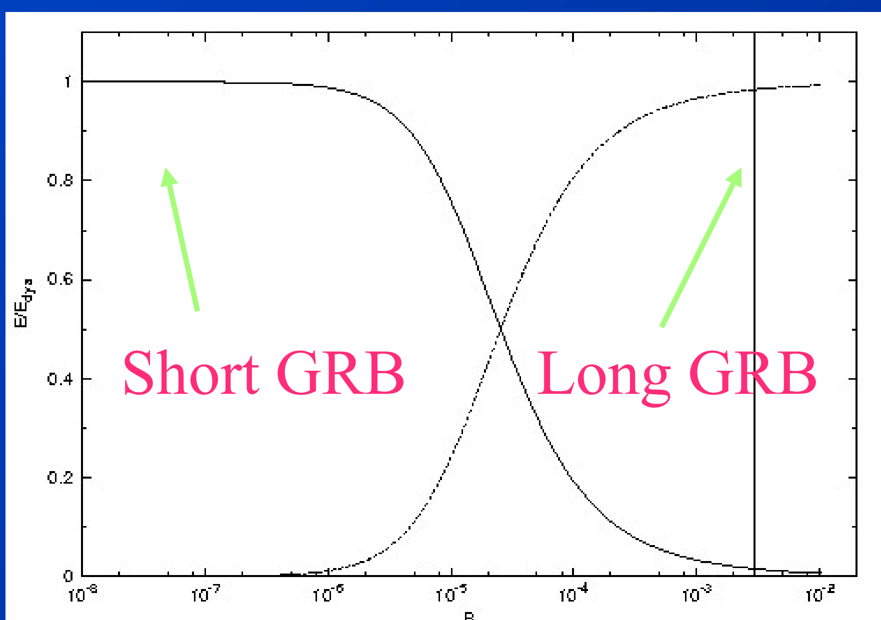

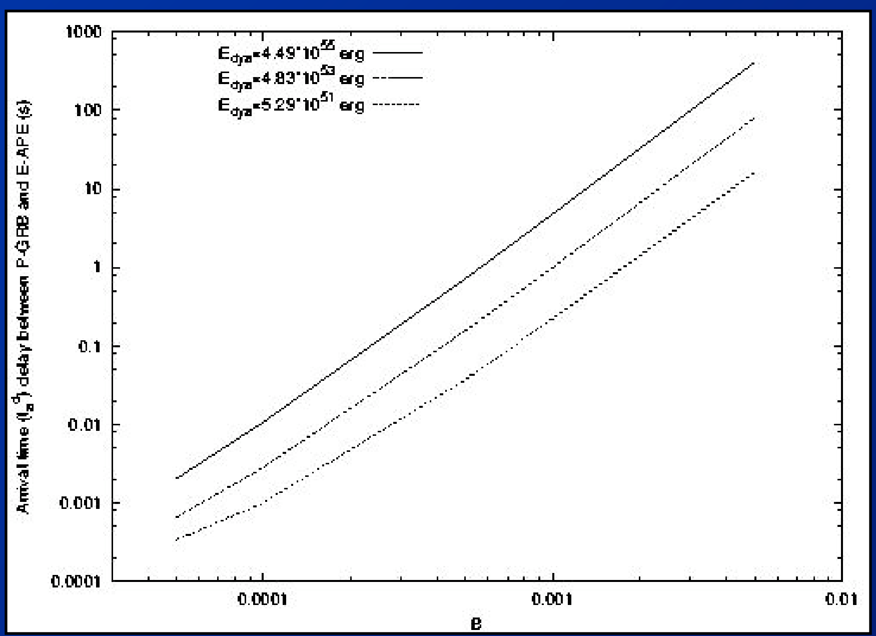

Temporal structure of GRB

Collision with baryonic remnant

Increase of opacity of pulse

Conversion of internal energy in kinetic energy

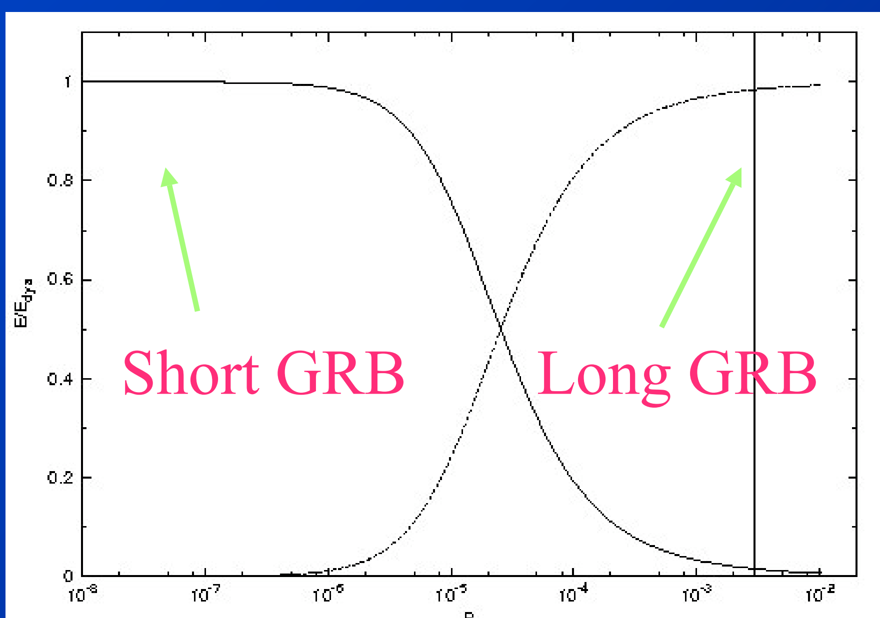

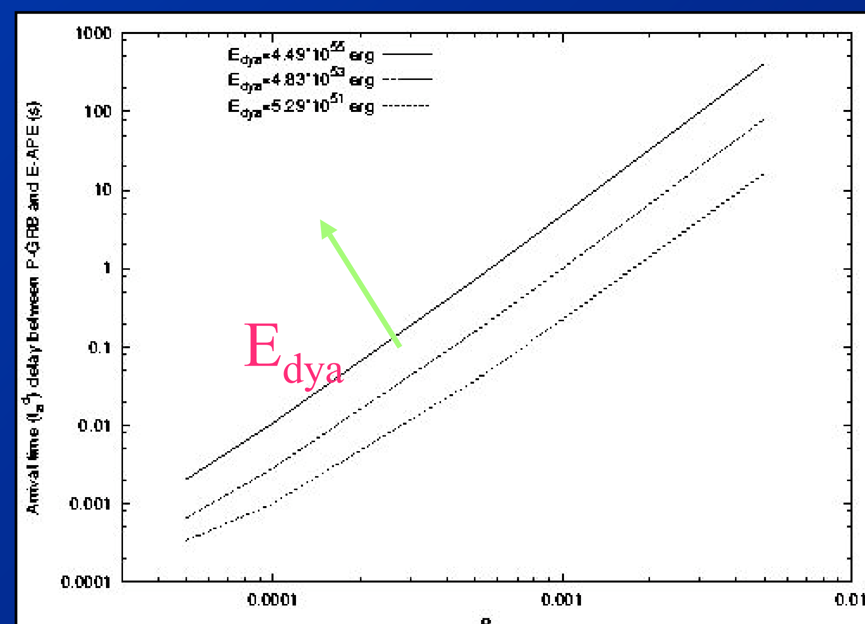

Ruffini R., Bianco C.L., Chardonnet P., Fraschetti F., Xue S.S., ApJ, 555, L113, 2001
Fraschetti F., GdA, 31/4, 14-18, 2005
Fraschetti F., JKPS, 42, S24, 2003

Equations for afterglow

In the laboratory system

Equations for afterglow

In the laboratory system

$$
\begin{cases}
\rho_{B_1}\gamma_1^{\,2}V_1 + \Delta M_{ism}c^2 = \left(\rho_{B_1}\dfrac{V_1}{V_2} + \dfrac{\Delta M_{ism}c^2}{V_2} + \Delta\varepsilon\right)\gamma_2^{\,2}V_2 \\
\rho_{B_1}\gamma_1 U_{r_1}V_1 = \left(\rho_{B_1}\dfrac{V_1}{V_2} + \dfrac{\Delta M_{ism}c^2}{V_2} + \Delta\varepsilon\right)\gamma_2 U_{r_2}V_2
\end{cases}
$$

Equations for afterglow

In the laboratory system

$$\begin{cases} \rho_{B_1}\gamma_1^{\,2}V_1 + \Delta M_{ism}c^2 = \left(\rho_{B_1}\dfrac{V_1}{V_2} + \dfrac{\Delta M_{ism}c^2}{V_2} + \Delta\varepsilon\right)\gamma_2^{\,2}V_2 \\ \rho_{B_1}\gamma_1 U_{r_1}V_1 = \left(\rho_{B_1}\dfrac{V_1}{V_2} + \dfrac{\Delta M_{ism}c^2}{V_2} + \Delta\varepsilon\right)\gamma_2 U_{r_2}V_2 \end{cases}$$

with

$$\begin{cases} \rho_B = \dfrac{\left(M_B + M_{ism}\right)c^2}{V} \\ M_{ism}(r) = m_p n_{ism}\dfrac{4\pi}{3}\left(r^3 - r_0^{\,3}\right) \\ U_r = \sqrt{\gamma^2 - 1} \end{cases}$$

Equations for afterglow

In the laboratory system

$$\begin{cases} \rho_{B_1}\gamma_1^{\,2}V_1 + \Delta M_{ism}c^2 = \left(\rho_{B_1}\dfrac{V_1}{V_2} + \dfrac{\Delta M_{ism}c^2}{V_2} + \Delta\varepsilon\right)\gamma_2^{\,2}V_2 \\ \rho_{B_1}\gamma_1 U_{r_1}V_1 = \left(\rho_{B_1}\dfrac{V_1}{V_2} + \dfrac{\Delta M_{ism}c^2}{V_2} + \Delta\varepsilon\right)\gamma_2 U_{r_2}V_2 \end{cases}$$

with

$$\begin{cases} \rho_B = \dfrac{(M_B + M_{ism})c^2}{V} \\ M_{ism}(r) = m_p n_{ism}\dfrac{4\pi}{3}\left(r^3 - r_0^{\,3}\right) \\ U_r = \sqrt{\gamma^2 - 1} \end{cases}$$

$$\begin{cases} \Delta\varepsilon = \rho_{B_1}\dfrac{V_1}{V_2}\sqrt{1 + 2\gamma_1\dfrac{\Delta M_{ism}c^2}{\rho_{B_1}V_1} + \left(\dfrac{\Delta M_{ism}c^2}{\rho_{B_1}V_1}\right)^2} - \rho_{B_1}\dfrac{V_1}{V_2}\left(1 + \dfrac{\Delta M_{ism}c^2}{\rho_{B_1}V_1}\right) \\ \gamma_2 = \dfrac{\gamma_1 + \dfrac{\Delta M_{ism}c^2}{\rho_{B_1}V_1}}{\sqrt{1 + 2\gamma_1\dfrac{\Delta M_{ism}c^2}{\rho_{B_1}V_1} + \left(\dfrac{\Delta M_{ism}c^2}{\rho_{B_1}V_1}\right)^2}} \end{cases}$$

Equations for afterglow

In the laboratory system

$$\begin{cases} \rho_{B_1}\gamma_1^{\,2}V_1 + \Delta M_{ism}c^2 = \left(\rho_{B_1}\dfrac{V_1}{V_2} + \dfrac{\Delta M_{ism}c^2}{V_2} + \Delta\varepsilon\right)\gamma_2^{\,2}V_2 \\ \rho_{B_1}\gamma_1 U_{r_1}V_1 = \left(\rho_{B_1}\dfrac{V_1}{V_2} + \dfrac{\Delta M_{ism}c^2}{V_2} + \Delta\varepsilon\right)\gamma_2 U_{r_2}V_2 \end{cases}$$

with

$$\begin{cases} \rho_B = \dfrac{(M_B + M_{ism})c^2}{V} \\ M_{ism}(r) = m_p n_{ism}\dfrac{4\pi}{3}\left(r^3 - r_0^{\,3}\right) \\ U_r = \sqrt{\gamma^2 - 1} \end{cases}$$

$$\begin{cases} \Delta\varepsilon = \rho_{B_1}\dfrac{V_1}{V_2}\sqrt{1 + 2\gamma_1\dfrac{\Delta M_{ism}c^2}{\rho_{B_1}V_1} + \left(\dfrac{\Delta M_{ism}c^2}{\rho_{B_1}V_1}\right)^2} - \rho_{B_1}\dfrac{V_1}{V_2}\left(1 + \dfrac{\Delta M_{ism}c^2}{\rho_{B_1}V_1}\right) \\ \gamma_2 = \dfrac{\gamma_1 + \dfrac{\Delta M_{ism}c^2}{\rho_{B_1}V_1}}{\sqrt{1 + 2\gamma_1\dfrac{\Delta M_{ism}c^2}{\rho_{B_1}V_1} + \left(\dfrac{\Delta M_{ism}c^2}{\rho_{B_1}V_1}\right)^2}} \end{cases}$$

$$\frac{\Delta M_{ism}c^2}{\rho_{B_1}V_1} \ll 1$$

Equations for afterglow

In the laboratory system

$$\begin{cases} \rho_{B_1}\gamma_1^2 V_1 + \Delta M_{ism}c^2 = \left(\rho_{B_1}\frac{V_1}{V_2} + \frac{\Delta M_{ism}c^2}{V_2} + \Delta\varepsilon\right)\gamma_2^2 V_2 \\ \rho_{B_1}\gamma_1 U_{r_1} V_1 = \left(\rho_{B_1}\frac{V_1}{V_2} + \frac{\Delta M_{ism}c^2}{V_2} + \Delta\varepsilon\right)\gamma_2 U_{r_2} V_2 \end{cases}$$

with

$$\begin{cases} \rho_B = \frac{(M_B + M_{ism})c^2}{V} \\ M_{ism}(r) = m_p n_{ism}\frac{4\pi}{3}\left(r^3 - r_0^3\right) \\ U_r = \sqrt{\gamma^2 - 1} \end{cases}$$

$$\begin{cases} \Delta\varepsilon = \rho_{B_1}\frac{V_1}{V_2}\sqrt{1 + 2\gamma_1\frac{\Delta M_{ism}c^2}{\rho_{B_1}V_1} + \left(\frac{\Delta M_{ism}c^2}{\rho_{B_1}V_1}\right)^2} - \rho_{B_1}\frac{V_1}{V_2}\left(1 + \frac{\Delta M_{ism}c^2}{\rho_{B_1}V_1}\right) \\ \gamma_2 = \frac{\gamma_1 + \frac{\Delta M_{ism}c^2}{\rho_{B_1}V_1}}{\sqrt{1 + 2\gamma_1\frac{\Delta M_{ism}c^2}{\rho_{B_1}V_1} + \left(\frac{\Delta M_{ism}c^2}{\rho_{B_1}V_1}\right)^2}} \end{cases}$$

$$\frac{\Delta M_{ism}c^2}{\rho_{B_1}V_1} \ll 1 \quad \longrightarrow \quad \begin{cases} dE_{int} = (\gamma - 1)dM_{ism}c^2 \\ d\gamma = -\frac{\gamma^2 - 1}{M_B + M_{ism}}dM_{ism} \end{cases}$$

Emitted luminosity

Thermal distribution of energy in comoving system:

Emitted luminosity

Thermal distribution of energy in comoving system:

$$\begin{cases} \dfrac{dE}{dt_a^d\, d\Omega} = \displaystyle\int_{EQTS} \dfrac{\Delta\varepsilon}{4\pi}\, v \Lambda^{-4} \cos\vartheta\, \dfrac{dt}{dt_a^d} W\left(\nu_1, \nu_2, T_{arr}\right) d\Sigma \\ t_a^d = \left(1+z\right)\left(t - \dfrac{\int_0^t v\left(t'\right) dt' + r_{ds}}{c} \cos\vartheta + \dfrac{r_{ds}}{c} \right) \end{cases}$$

Emitted luminosity

Thermal distribution of energy in comoving system:

$$\begin{cases} \dfrac{dE}{dt_a^d \, d\Omega} = \displaystyle\int_{EQTS} \dfrac{\Delta\varepsilon}{4\pi} \, v \, \Lambda^{-4} \cos\vartheta \, \dfrac{dt}{dt_a^d} \boxed{W\left(\nu_1, \nu_2, T_{arr}\right)} d\Sigma \\ t_a^d = (1+z)\left(t - \dfrac{\int_0^t v(t') dt' + r_{ds}}{c} \cos\vartheta + \dfrac{r_{ds}}{c} \right) \end{cases}$$

Emitted luminosity

Thermal distribution of energy in comoving system:

$$
\begin{cases}
\dfrac{dE}{dt_a^d\, d\Omega} = \int_{EQTS} \dfrac{\Delta\varepsilon}{4\pi}\, v\Lambda^{-4} \cos\vartheta\, \dfrac{dt}{dt_a^d}\, W(\nu_1, \nu_2, T_{arr})\, d\Sigma \\
t_a^d = (1+z)\left(t - \dfrac{\int_0^t v(t')\,dt' + r_{ds}}{c} \cos\vartheta + \dfrac{r_{ds}}{c} \right)
\end{cases}
$$

$$
W(\nu_1, \nu_2, T_{arr}) = \frac{2}{aT_{arr}^{4}{}^{3}} \int_{\nu_1}^{\nu_2} \frac{h\nu}{e^{h\nu/(kT_{arr})} - 1}\, d\left(\frac{h\nu}{c}\right)^3
$$

Emitted luminosity

Thermal distribution of energy in comoving system:

$$
\begin{cases}
\dfrac{dE}{dt_a^d\, d\Omega} = \displaystyle\int_{EQTS} \frac{\Delta\varepsilon}{4\pi}\, v \Lambda^{-4} \cos\vartheta\, \frac{dt}{dt_a^d}\, W\left(\nu_1, \nu_2, T_{arr}\right) d\Sigma \\
t_a^d = (1+z)\left(t - \dfrac{\int_0^t v(t')\,dt' + r_{ds}}{c} \cos\vartheta + \dfrac{r_{ds}}{c} \right)
\end{cases}
$$

$$
W\left(\nu_1, \nu_2, T_{arr}\right) = \frac{2}{a T_{arr}^4 h^3} \int_{\nu_1}^{\nu_2} \frac{h\nu}{e^{h\nu/(kT_{arr})} - 1}\, d\left(\frac{h\nu}{c}\right)^3
$$

T_{arr} is the temperature of radiation emitted by $d\Sigma$ and observed on the Earth

Temporal substructure of peak

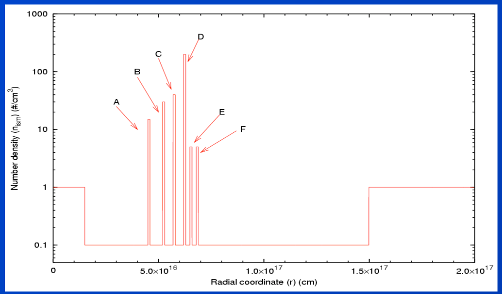

Peak	r (cm)	τ (s)	t (s)	t_a (s)	t_a^d (s)	Δt_a^d (s)	γ	"Superluminal" $v \equiv \frac{r}{t_a^d}$
A	4.50×10^{16}	4.88×10^3	1.50×10^6	7.90	15.8	0.400	303.8	$9.5 \times 10^4 c$
B	5.20×10^{16}	5.74×10^3	1.73×10^6	9.50	19.0	0.622	265.4	$9.1 \times 10^4 c$
C	5.70×10^{16}	6.54×10^3	1.90×10^6	11.4	22.9	1.13	200.5	$8.3 \times 10^4 c$
D	6.20×10^{16}	7.64×10^3	2.07×10^6	15.0	30.1	5.16	139.9	$6.9 \times 10^4 c$
E	6.50×10^{16}	9.22×10^3	2.17×10^6	27.9	55.9	10.2	57.23	$3.9 \times 10^4 c$
F	6.80×10^{16}	1.10×10^4	2.27×10^6	43.7	87.4	10.6	56.24	$2.6 \times 10^4 c$

Temporal substructure of peak

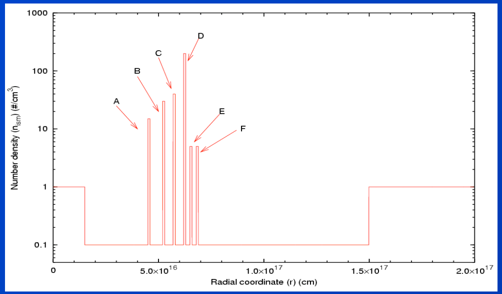

Peak	r (cm)	Δt_a^d (s)	γ	"Superluminal" $v \equiv \frac{r}{t_a^d}$
A	4.50×10^{16}	0.400	303.8	$9.5 \times 10^4 c$
B	5.20×10^{16}	0.622	265.4	$9.1 \times 10^4 c$
C	5.70×10^{16}	1.13	200.5	$8.3 \times 10^4 c$
D	6.20×10^{16}	5.16	139.9	$6.9 \times 10^4 c$
E	6.50×10^{16}	10.2	57.23	$3.9 \times 10^4 c$
F	6.80×10^{16}	10.6	56.24	$2.6 \times 10^4 c$

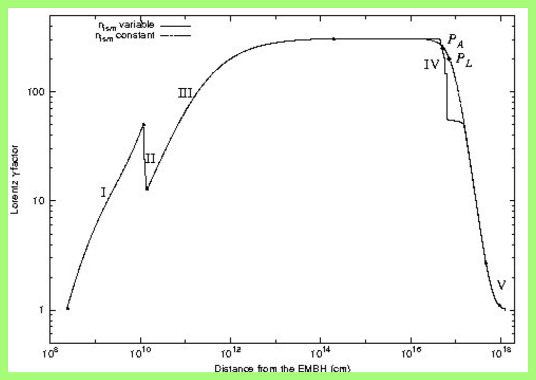

Temporal substructure of peak

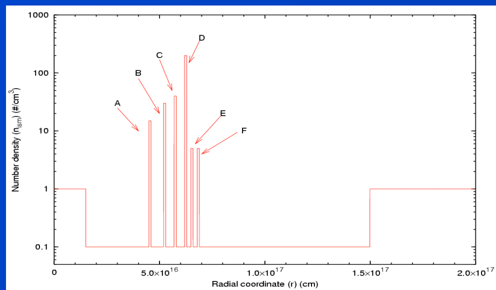

Peak	r (cm)	Δt_a^d (s)	γ	"Superluminal" $v \equiv \frac{r}{t_a^d}$
A	4.50×10^{16}	0.400	303.8	$9.5 \times 10^4 c$
B	5.20×10^{16}	0.622	265.4	$9.1 \times 10^4 c$
C	5.70×10^{16}	1.13	200.5	$8.3 \times 10^4 c$
D	6.20×10^{16}	5.16	139.9	$6.9 \times 10^4 c$
E	6.50×10^{16}	10.2	57.23	$3.9 \times 10^4 c$
F	6.80×10^{16}	10.6	56.24	$2.6 \times 10^4 c$

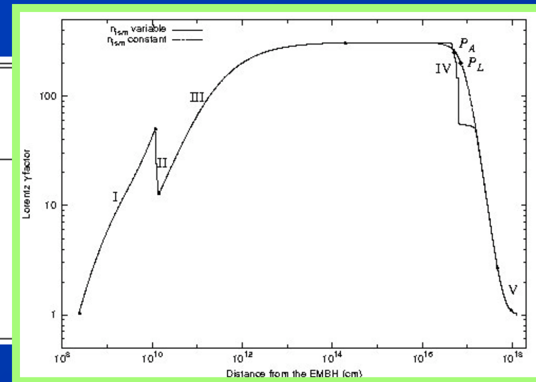

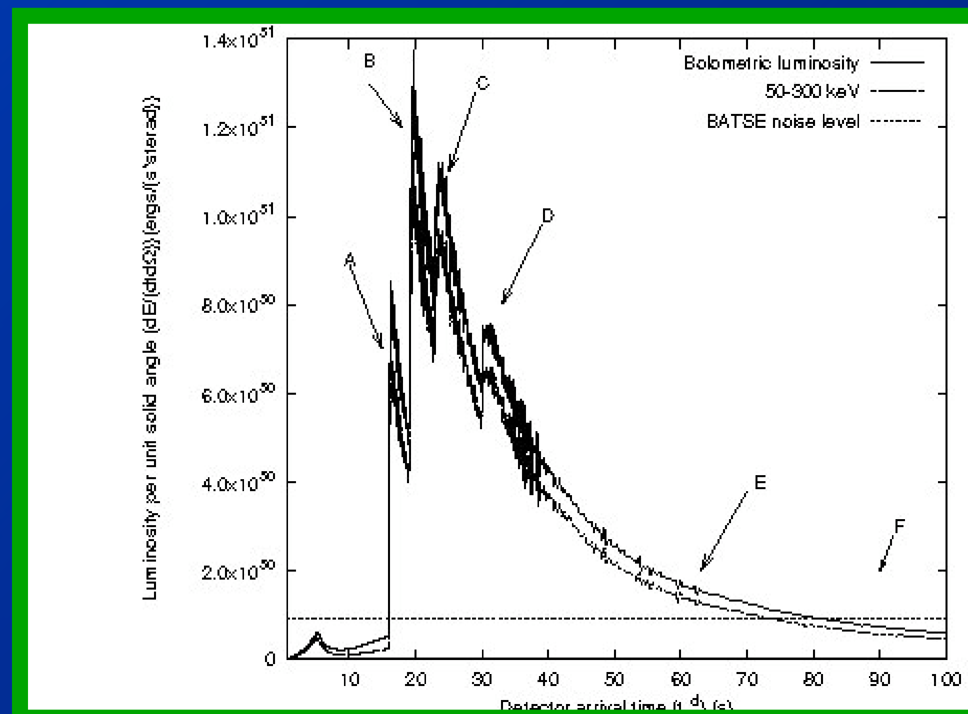

Temporal substructure of peak

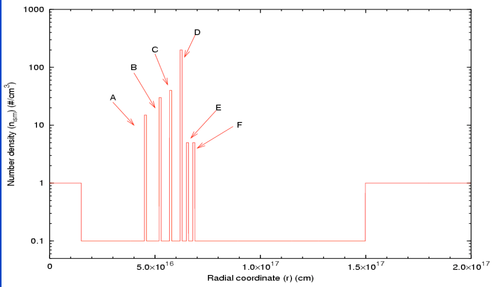

Peak	r (cm)	Δt_a^d (s)	γ	"Superluminal" $v \equiv \frac{r}{t_a^d}$
A	4.50×10^{16}	0.400	303.8	$9.5 \times 10^4 c$
B	5.20×10^{16}	0.622	265.4	$9.1 \times 10^4 c$
C	5.70×10^{16}	1.13	200.5	$8.3 \times 10^4 c$
D	6.20×10^{16}	5.16	139.9	$6.9 \times 10^4 c$
E	6.50×10^{16}	10.2	57.23	$3.9 \times 10^4 c$
F	6.80×10^{16}	10.6	56.24	$2.6 \times 10^4 c$

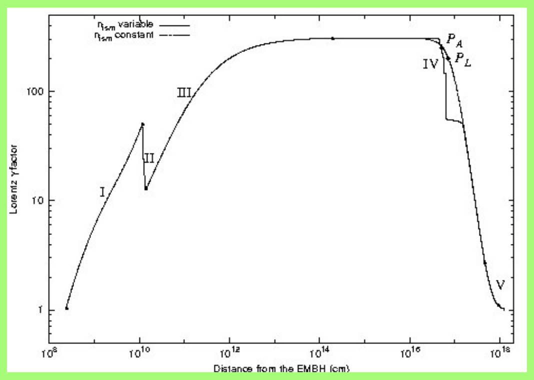

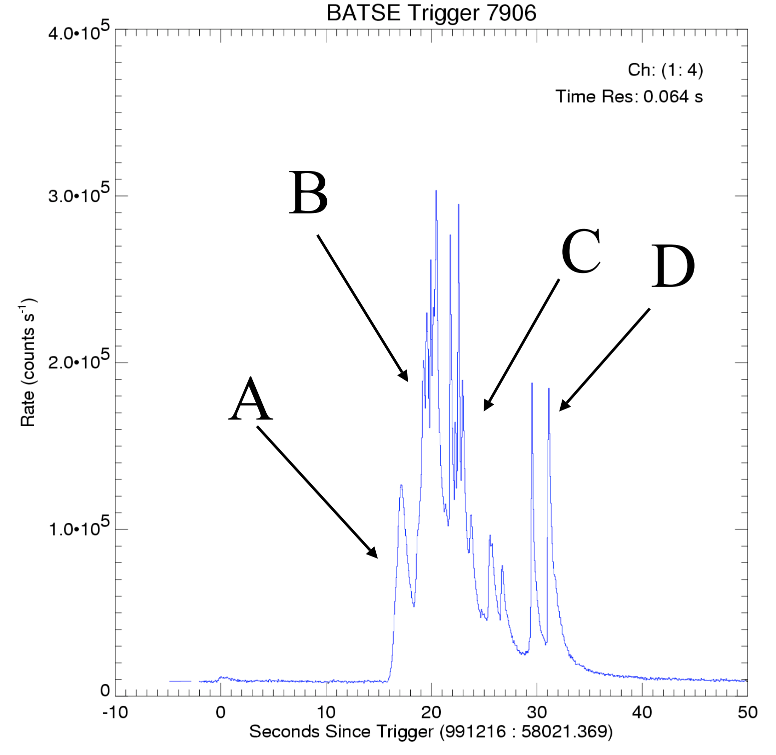

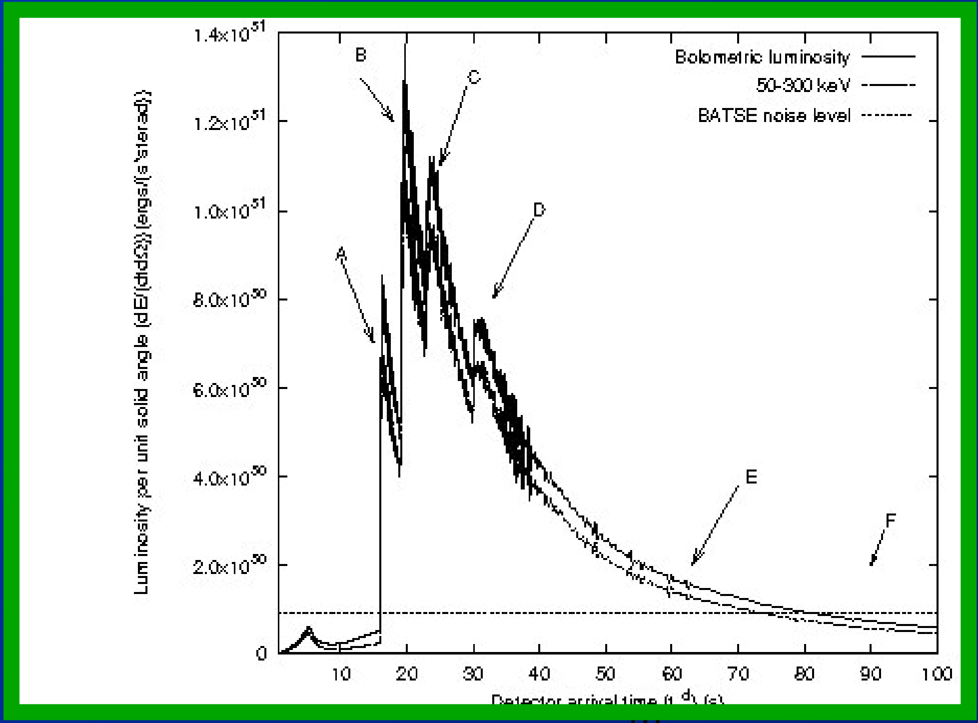

Ruffini R., Bianco C.L., Chardonnet P., **Fraschetti F.**, Xue S.S., ApJ, 555, L113, 2001
Ruffini R., Bianco C.L., Chardonnet P., **Fraschetti F.**, Xue S.S., IJMPD, 13, 5, 843, 2004

Spectral evolution

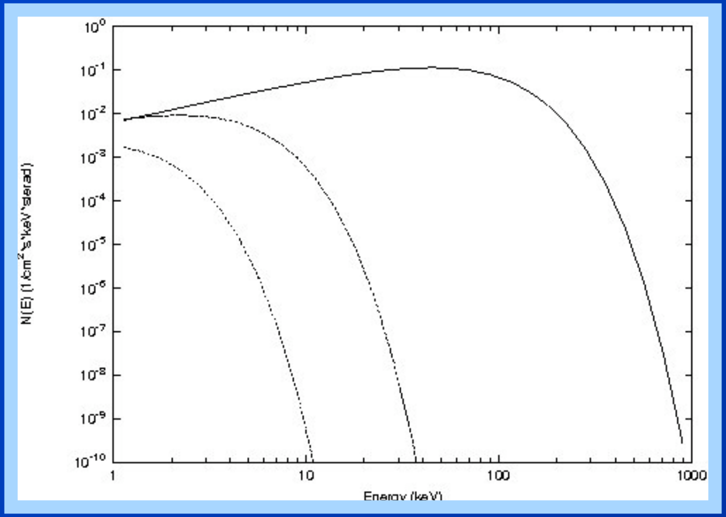

Spectral evolution

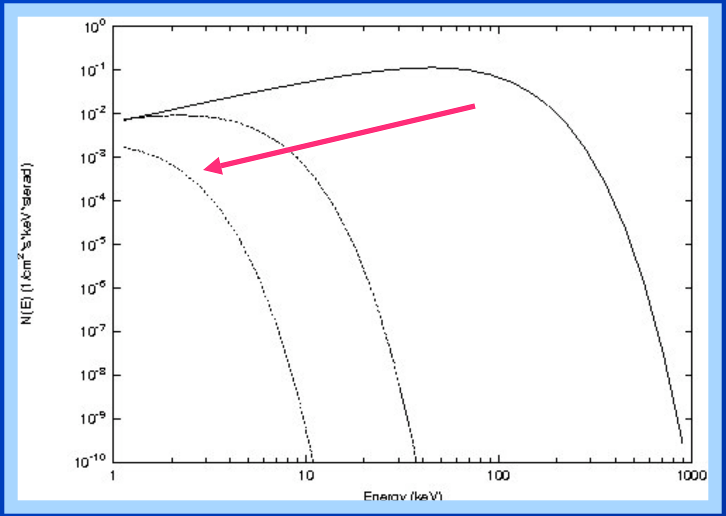

Hard-to-Soft evolution

Spectral evolution

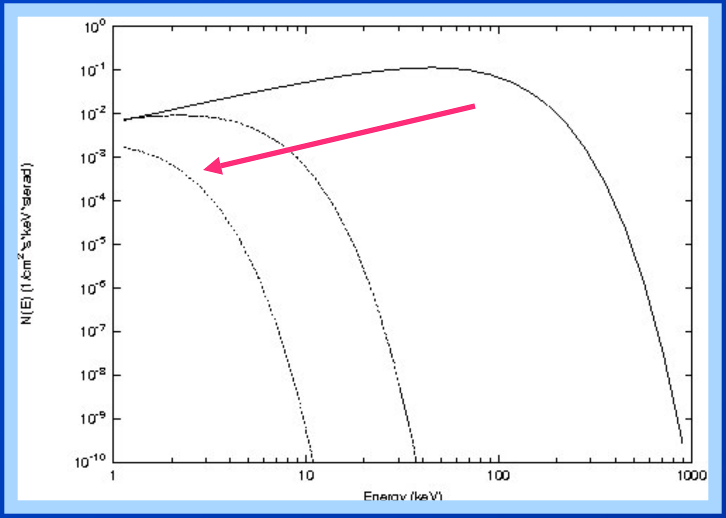

Hard-to-Soft evolution

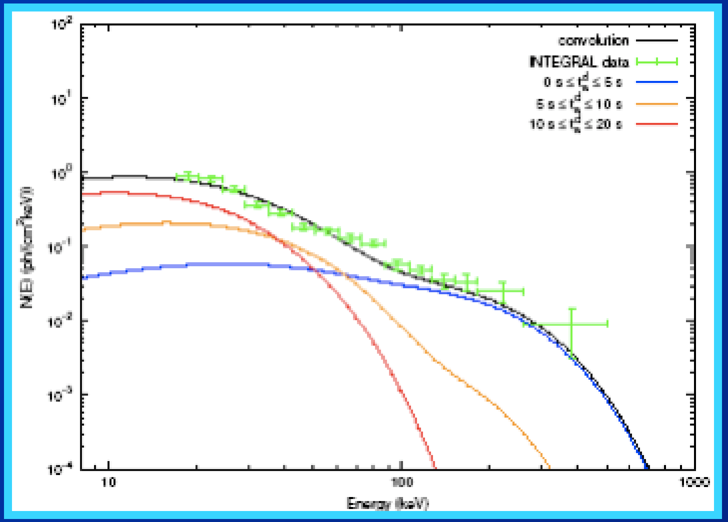

Time integrated spectrum

Spectral evolution

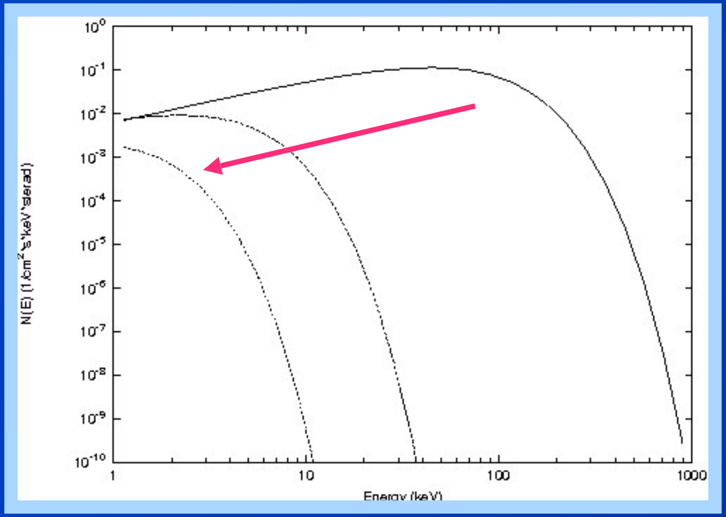

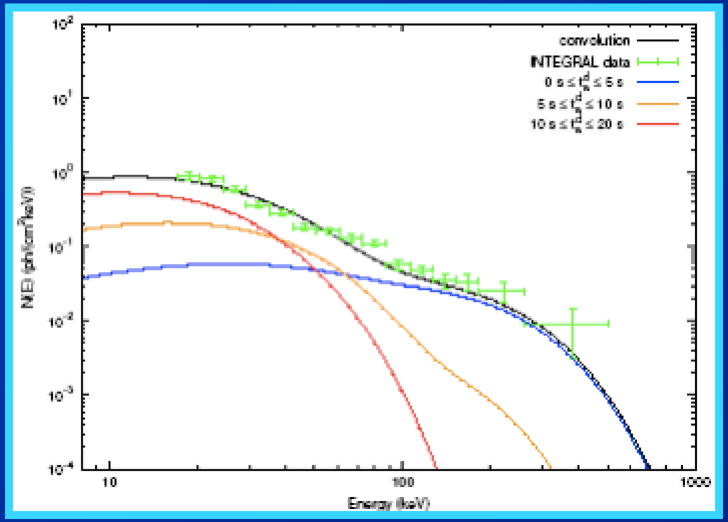

Hard-to-Soft evolution

Time integrated spectrum

Non-thermal observed spectrum

Spectral evolution

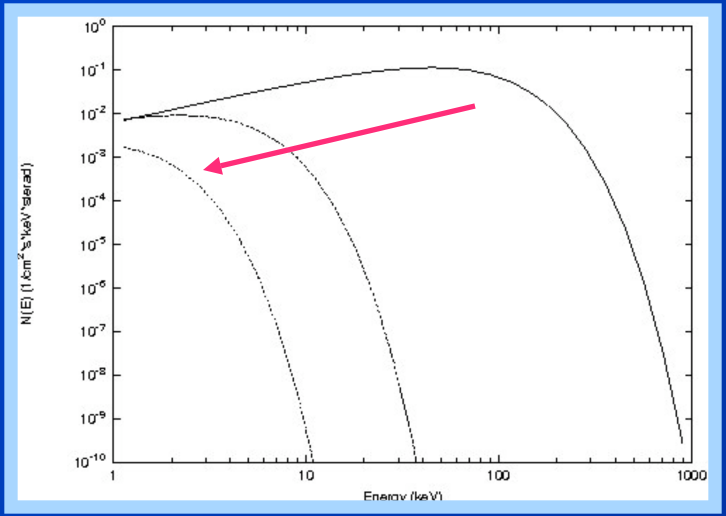

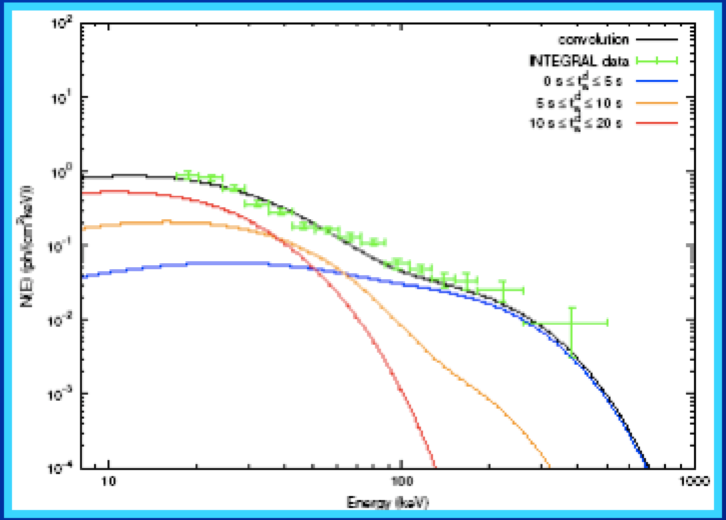

Hard-to-Soft evolution

Time integrated spectrum

Non-thermal observed spectrum

GRB 980425, 030329, 031203, 980519, 970228,…

Bernardini M.G., Bianco C.L., Chardonnet P., **Fraschetti F.**, Ruffini R., Xue S.S., ApJ, 634, L29, 2005

Swift era

Model verified in a precedently unobserved temporal window (10^2 -10^4 sec)

Structure of light curve afterglow simply explained the claimed breaks in light curves

Swift era

Model verified in a precedently unobserved temporal window (10^2 - 10^4 sec)

Structure of light curve afterglow simply explained the claimed breaks in light curves

GRB050315

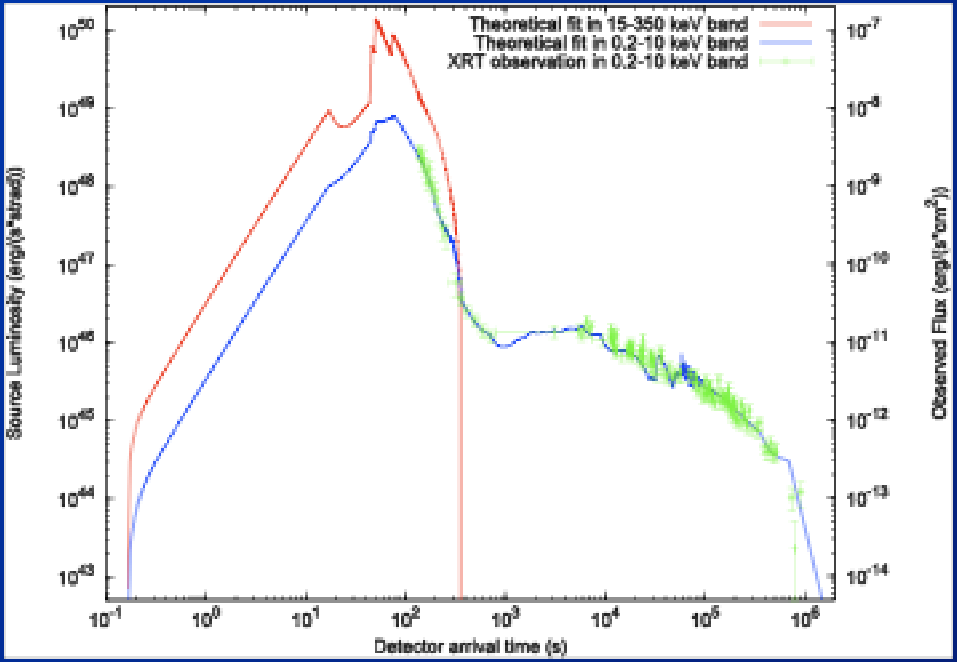

Ruffini R., Bernardini M.G., Bianco C.L., Chardonnet P., **Fraschetti F.**, Guida R., Xue S.S., ApJ, 645, L109, 2006

Light curve and spectrum of P-GRB

Evolution of sub slab to transparency

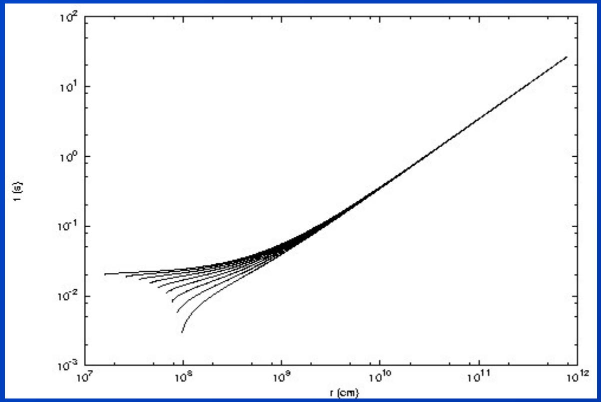

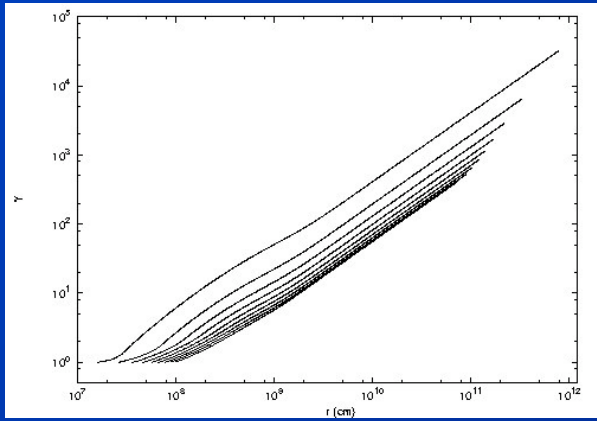

No internal shock

Light curve and spectrum of P-GRB

Evolution of sub slab to transparency

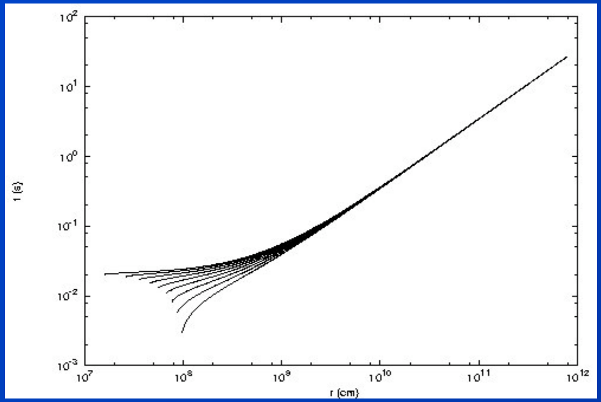

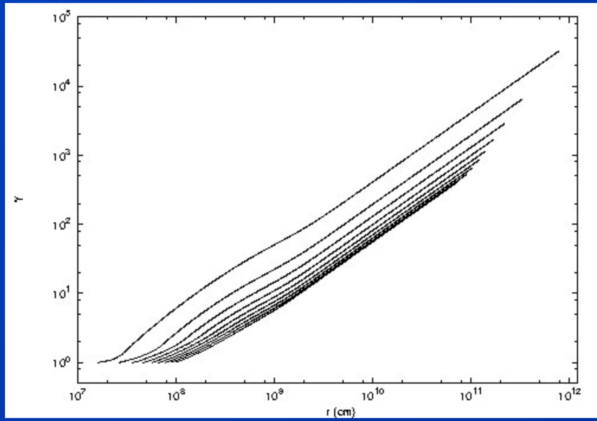

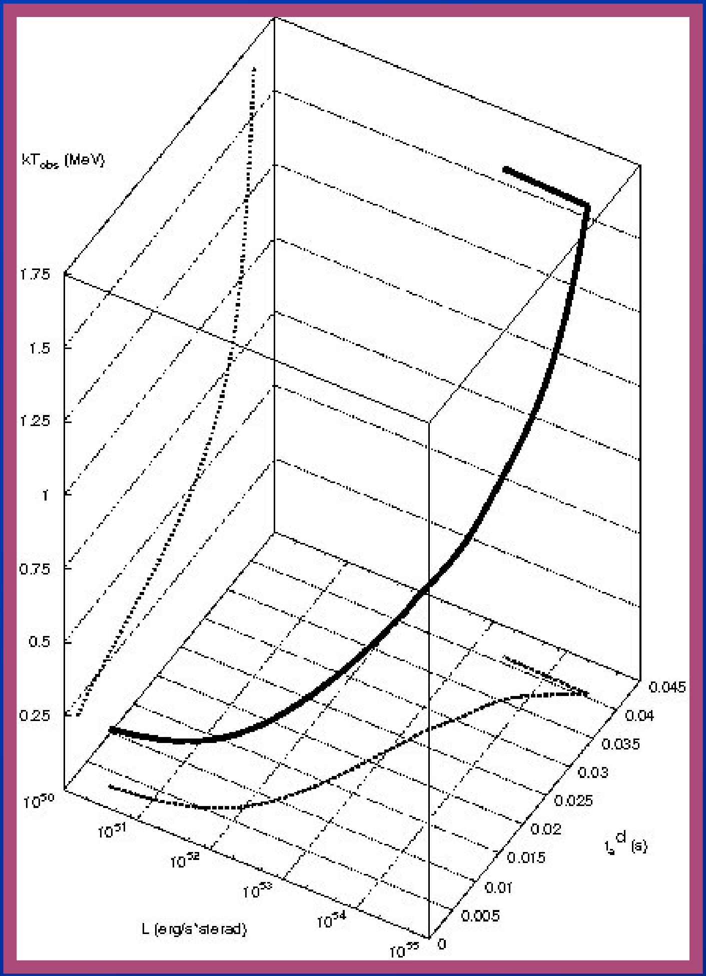

No internal shock

Light curve and spectrum of P-GRB

Evolution of sub slab to transparency

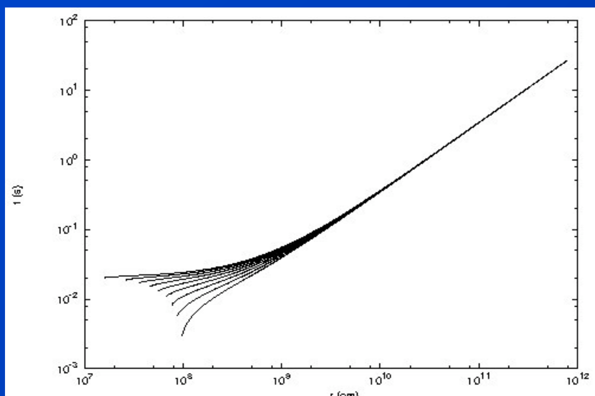

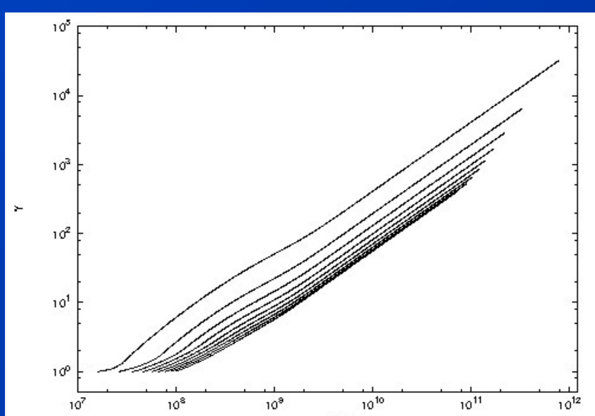

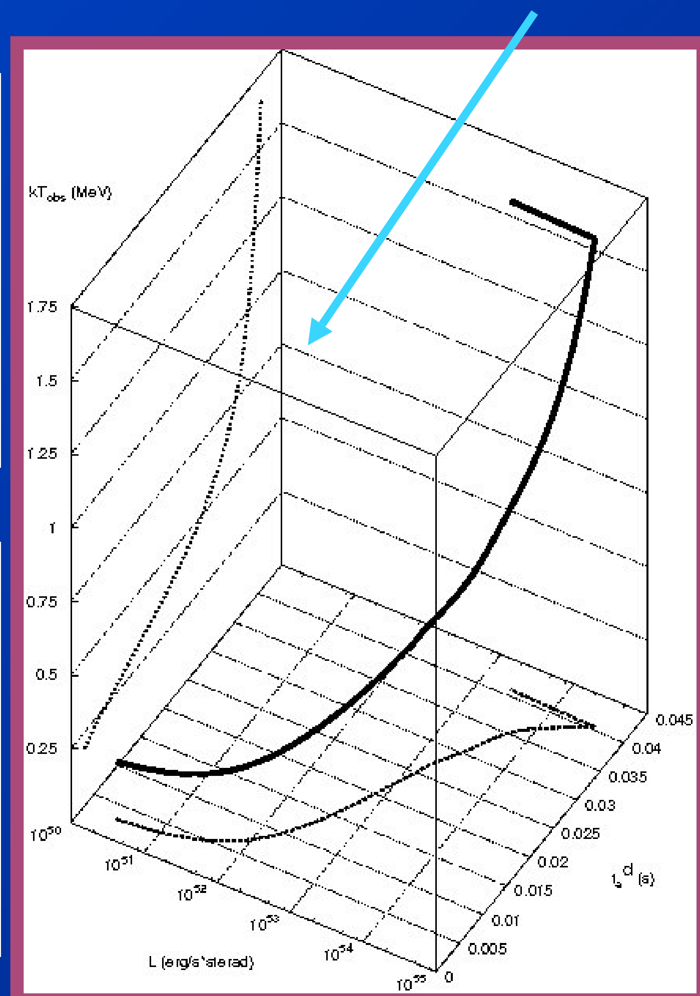

No internal shock

Light curve and spectrum of P-GRB

Evolution of sub slab to transparency

Soft-to-Hard

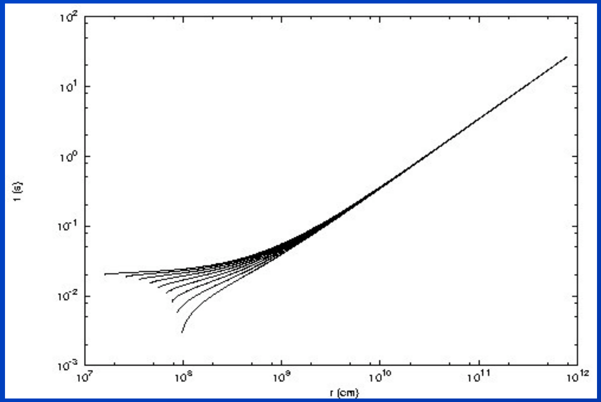

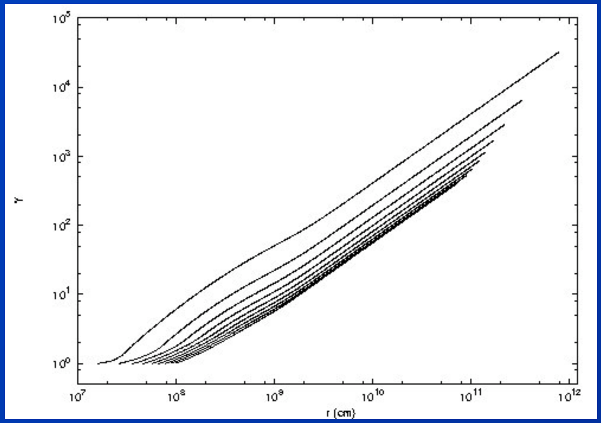

No internal shock

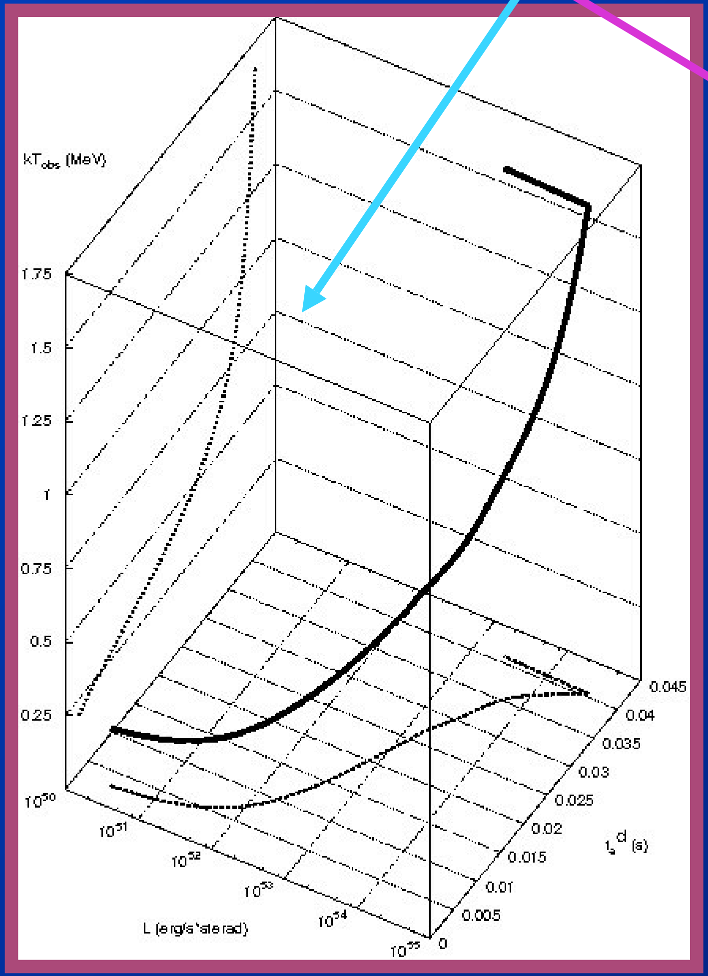

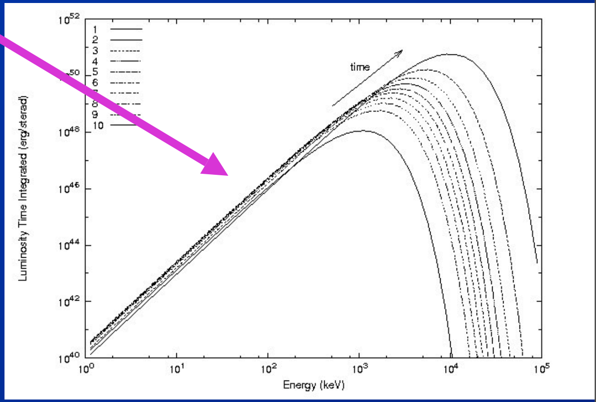

Light curve and spectrum of P-GRB

Evolution of sub slab to transparency

Soft-to-Hard

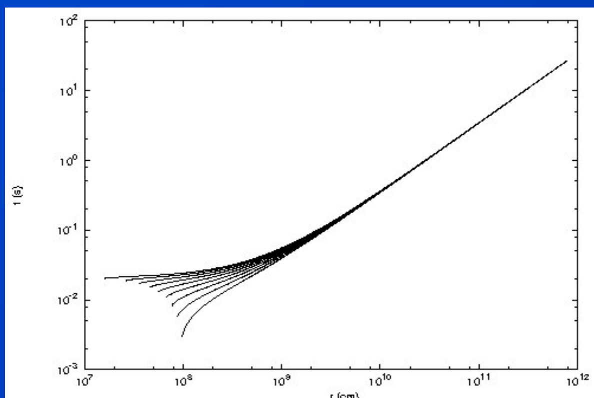

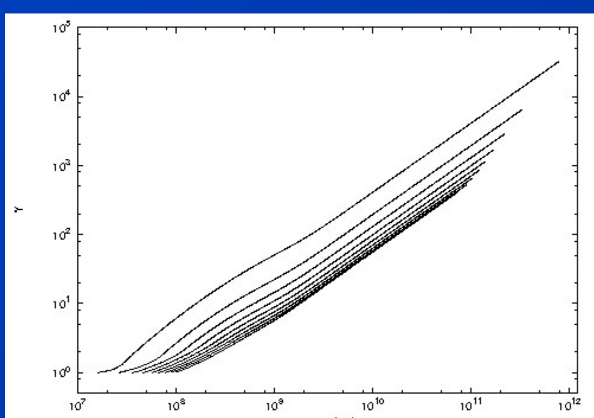

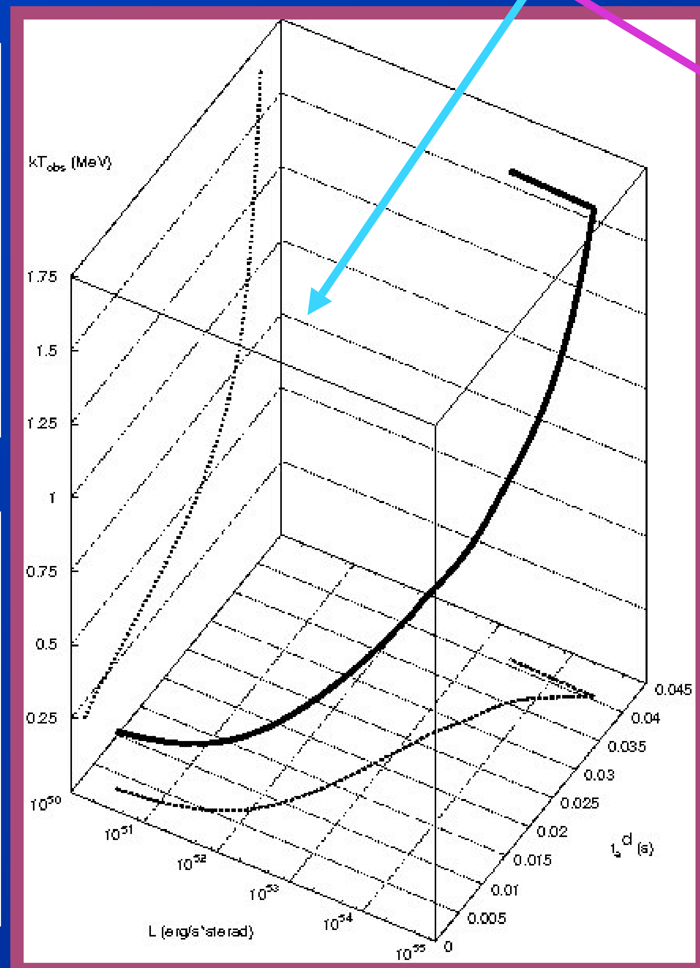

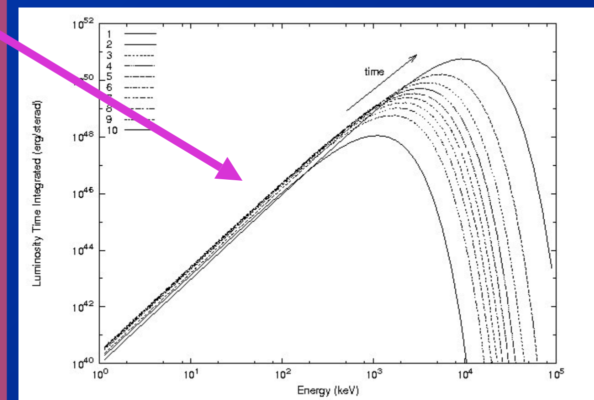

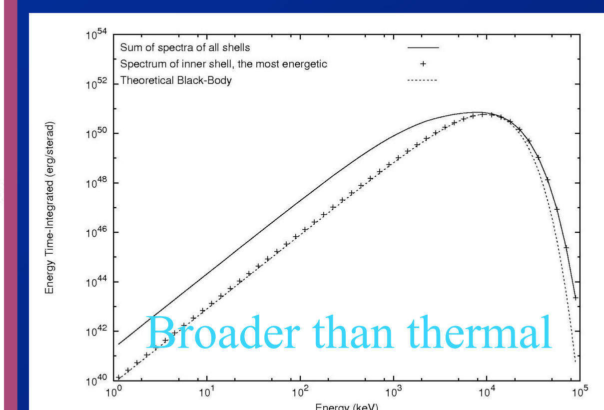

Broader than thermal

No internal shock

Ruffini R., Fraschetti F., Vitaglaino L., Xue S.S., IJMPD, 14, 1, 131, 2005

Conclusions

- The model presented builds the whole temporal evolution of the GRB, from the progenitor to the non-relativistic phase of the afterglow.
- Interpretation of temporal structure of GRB: P-GRB e E-APE.
- The condition “fully radiative” agrees with observations.
- The temporal variability of light curve traces the inhomogeneities of ISM.
- Observations are compatible with thermal spectrum in pulse comoving system.
- Agreement with Swift observations over a time interval of 10^6 sec.
- Spectral predictions for short bursts.